STUDY TO DEVELOP IMPROVED SPACECRAFT SNOW SURVEY METHODS USING SKYLAB/EREP DATA

ERT Document No. 0412-F
Final Report

May 1975

Contract No. NAS 9-13305

JAMES C. BARNES
MICHAEL D. SMALLWOOD
JAMES L. COGAN

prepared for
PRINCIPAL INVESTIGATOR OFFICE
NATIONAL AERONAUTICS AND SPACE ADMINISTRATION
LYNDON B. JOHNSON SPACE CENTER
HOUSTON, TEXAS 77958

ENVIRONMENTAL RESEARCH & TECHNOLOGY, INC.
696 VIRGINIA ROAD CONCORD, MASSACHUSETTS 01742 (617) 369-8910

1. Report No.	2. Government Accession No.	3. Recipient's Catalog No.

4. Title and Subtitle	5. Report Date
Study to Develop Improved Spacecraft Snow Survey Methods Using Skylab/EREP Data	May 1975
	6. Performing Organization Code
7. Author(s) James C. Barnes, Michael D. Smallwood, and James L. Cogan	8. Performing Organization Report No. 0412-F
	10. Work Unit No.
9. Performing Organization Name and Address Environmental Research & Technology, Inc. 696 Virginia Road Concord, Massachusetts · 01742	11. Contract or Grant No. NAS9-13305
	13. Type of Report and Period Covered Type III - Final Report March 1973 - May 1975
12. Sponsoring Agency Name and Address National Aeronautics and Space Administration Lyndon B. Johnson Space Center Houston, Texas 77058	14. Sponsoring Agency Code

15. Supplementary Notes

Technical Monitor: Mr. Larry B. York
Principal Investigator Office
NASA Johnson Space Center

16. Abstract

The purpose of this investigation was to evaluate Skylab EREP data for mapping snowcover. Visual interpretation of photographs from the S190A Multispectral Camera and the S190B Earth Terrain Camera was performed to identify and map snowcovered areas. Data from the S192 Multispectral Scanner, S193 Scatterometer-Radiometer, and S194 L-Band Radiometer were then analyzed and compared with the photographs and other ground-truth information to determine how much additional information on snowcover could be derived from the measurements made in various portions of the spectrum. The results of the analysis of the S192 data have particular application to snow mapping. Two potential uses of measurements in the near-infrared spectral region are possible: (1) the use of a near-infrared band in conjunction with a visible band to distinguish automatically between snow and water droplet clouds; and (2) the use of one or more near-infrared bands to detect areas of melting snow.

17. Key Words (Suggested by Author(s))	18. Distribution Statement
Skylab/EREP Data Snow Mapping Snow Survey Methods	

19. Security Classif. (of this report)	20. Security Classif. (of this page)	21. No. of Pages	22. Price*
Unclassified	Unclassified	92	

*For sale by the Clearinghouse for Federal Scientific and Technical Information
Springfield, Virginia 22151

PAGE INTENTIONALLY BLANK

FOREWARD

This report was prepared for the National Aeronautics and Space Administration/Johnson Space Center by Environmental Research & Technology, Inc., under Contract No. NAS9-13305.

The authors wish to acknowledge the assistance of Mr. Larry B. York, of the Principal Investigations Management Office at NASA/Johnson Space Center, who was the Technical Monitor of the contract. The Skylab and Landsat data were provided by NASA/Johnson Space Center and NASA/Goddard Space Flight Center, respectively. The aircraft photography was provided by the NASA/Ames Research Center Earth Resources Aircraft Project; the Salt River Project Office in Phoenix provided the aerial snow charts, and the USDA's Rocky Mountain Forest and Range Experiment Station provided information concerning the Beaver Creek Watershed Project in Arizona. The cooperation of each of these agencies is appreciated.

PAGE INTENTIONALLY BLANK

ABSTRACT

The purpose of this investigation was to evaluate Skylab EREP data for mapping snowcover. Visual interpretation of photographs from the S190A Multispectral Camera and the S190B Earth Terrain Camera was performed to identify and map snowcovered areas. Data from the S192 Multispectral Scanner, S193 Scatterometer-Radiometer, and S194 L-Band Radiometer were then analyzed and compared with the photographs to determine how much additional information on snowcover could be derived from the measurements made in various portions of the spectrum. The Skylab EREP data were also compared with aircraft photography, imagery from the Landsat satellite, and other ground truth information including aerial snow survey charts and standard snow depth reports.

The results of the investigation will assist in the development of improved satellite sensors to map snowcover that will lead to a more efficient and cost effective means for collecting snow data for use in runoff prediction and water management programs. In particular, the S192 Multispectral Scanner data have provided for the first time an opportunity to examine the reflectance characteristics of snowcover in several spectral bands extending from the visible into the near-infrared spectral region to about 2 μm. The analysis of the S192 imagery and digital tape data indicates a sharp drop in reflectance of snow in the near-infrared, with snow becoming essentially non-reflective in Bands 11 (1.55-1.75 μm) and 12 (2.10-2.35 μm). The results are in good agreement with the results of laboratory experiments. Two potential applications to snow mapping of measurements in the near-infrared spectral region are possible: (1) the use of a near-infrared band in conjunction with a visible band to distinguish automatically between snow and water droplet clouds; and (2) the use of one or more near-infrared bands to detect areas of melting snow.

PAGE INTENTIONALLY BLANK

TABLE OF CONTENTS

LIST OF ILLUSTRATIONS

LIST OF TABLES

PAGE INTENTIONALLY BLANK

1. INTRODUCTION

1.1 Purpose of Investigation

The purpose of this investigation was to evaluate Skylab EREP data for mapping snowcover. Visual interpretation of photographs from the S190A Multispectral Camera and the S190B Earth Terrain Camera was performed to identify and map snowcovered areas. Data from the S192 Multispectral Scanner, S193 Scatterometer-Radiometer, and S194 L-Band Radiometer were then analyzed and compared with the photographs to determine how much additional information on snowcover could be derived from the measurements made in various portions of the spectrum. The Skylab EREP data were also compared with aircraft photography, imagery from the Landsat satellite, and other ground truth information including aerial snow survey charts and standard snow depth reports. The results of this investigation will assist in the development of improved satellite sensors to map snowcover that will lead to a more efficient and cost effective means for collecting snow data for use in runoff prediction and water management programs.

1.2 Applications of Satellite Observations to Snow Mapping

One of the first "earth resources" applications of satellite observations was to map snow and ice. More than ten years ago studies were underway to map snow using meteorological satellite images. Even at that time it was realized that the relatively crude-resolution imagery could, nevertheless, provide useful information on the extent of the earth's snowcover.

Since then, as improved satellite systems have been developed, an increasing use has been made of remote sensing from space to monitor snowcover. Quasi-operational use in snow hydrology is currently being made of the NOAA satellite Very High Resolution Radiometer imagery, and the data from the Landsat (formerly ERTS) satellite has been shown to have substantial practical application for snow mapping. A summary report on the status of satellite snow survey was prepared by an international committee for the World Meteorological Organization (McClain, 1973); recently, a handbook of techniques for satellite snow mapping has

been prepared (Barnes and Bowley, 1974) to assist NASA Goddard Space Flight Center in the planning of a practical demonstration of the application of satellite data to snow hydrology.

Additional references pertaining to the use of NOAA satellite data include Wiesnet (1974) and McGinnis, Pritchard, and Wiesnet (1975); references pertaining to the application of Landsat data include: Barnes, Bowley, and Simmes (1974); Bowley and Barnes (1975); Meier (1973); and Rango, Salomonson, and Foster (1975). A snow mapping experiment was also conducted as part of the Skylab-4 Visual Observations Project; the report describing that experiment is currently in publication (Barnes, et al 1975).

1.3 Economic Impact of Accurate Snowcover Measurements

Snowcover greatly affects the large-scale geophysical environment of the earth, influencing both the heat balance at the surface and the worldwide water balance. Moreover, in many parts of the world, snow has an enormous economic impact; in the Western United States, much of the available water comes from mountain snowpacks.

Although it is difficult to assess in exact dollar amounts the economic value of accurate streamflow forecasting and of snow survey data, estimates have been made for some areas. In a discussion at the Interdisciplinary Symposium on Advanced Concepts and Techniques in the Study of Snow and Ice Resources, held in Monterey, California, in December 1973, it was pointed out that accurate streamflow forecasting is probably worth as much as 40 million dollars a year to the State of California; since snowmelt accounts for a large percentage of the total streamflow, the importance of snow data as input to runoff models is obvious. In the same discussion, it was mentioned that the value of snow survey data in the Pacific Northwest has been determined more directly; the results of a study of three drainage basins showed that the annual benefit from the addition of snow survey data to streamflow forecasting schemes was 385 thousand dollars. Meier (1973) refers to a National Academy of Sciences panel report, which states "in mountainous areas of the United States, millions of dollars are spent each year at fixed locations to measure snowpack for forecast purposes; improved forecasts are estimated to be worth 10^7 to 10^8 dollars per year to water users in the western United States alone".

2. TEST SITE AREAS

2.1 Locations of Test Site Areas

Five test site areas were originally specified for the investigation; four of the sites are in mountainous areas of the western United States and one in the area of relatively flat terrain in the north-central part of the country. The sites in the western mountains were selected because each has characteristically different terrain, forest cover, and snowfall climatologies. The test site areas, which are shown in the map in Figure 2-1 are as follows: No. 318107, southern Sierra Nevada in California; No. 318108, Cascades in Washington and Oregon; No. 318191, Upper Columbia Basin in Idaho and western Montana; No. 318208, Salt-Verde Watershed in Arizona; and No. 318592, the Upper Mississippi-Missouri River Basin region. In each of these areas snowmelt runoff is an important hydrologic consideration.

In addition to the test site areas specified for this investigation, one test site of another Skylab/EREP investigation being conducted at Environmental Research & Technology, Inc. (EPN No. 439) also included mountainous terrain for which EREP data viewing snowcover were collected. This additional test site, which covers the central Utah area near Great Salt Lake, is also indicated in Figure 2-1 (Site 547220).

2.2 Description of Test Site Areas

Of the specified test site areas, useful Skylab data were collected for Site 318107 on the SL-2 mission (EREP Pass 3) and on the SL-4 mission (Pass 98), for Site 547220 on the SL-2 mission (Pass 5), for Site 318208 on the SL-4 mission (Pass 83), and for Site 318592 on the SL-4 mission (Passes 83, 89, and 90). Because of cloud obscuration only a limited amount of data were collected for Site 318108 (SL-2 mission, Pass 8), and no data were collected for Site 318191. The availability of data from both the first and third missions presented an opportunity to analyze measurements collected over snowcover representative of late spring conditions (June 1973) and mid-winter conditions (January-February 1974). Descriptions of the test site areas for which data were analyzed are given in the following paragraphs.

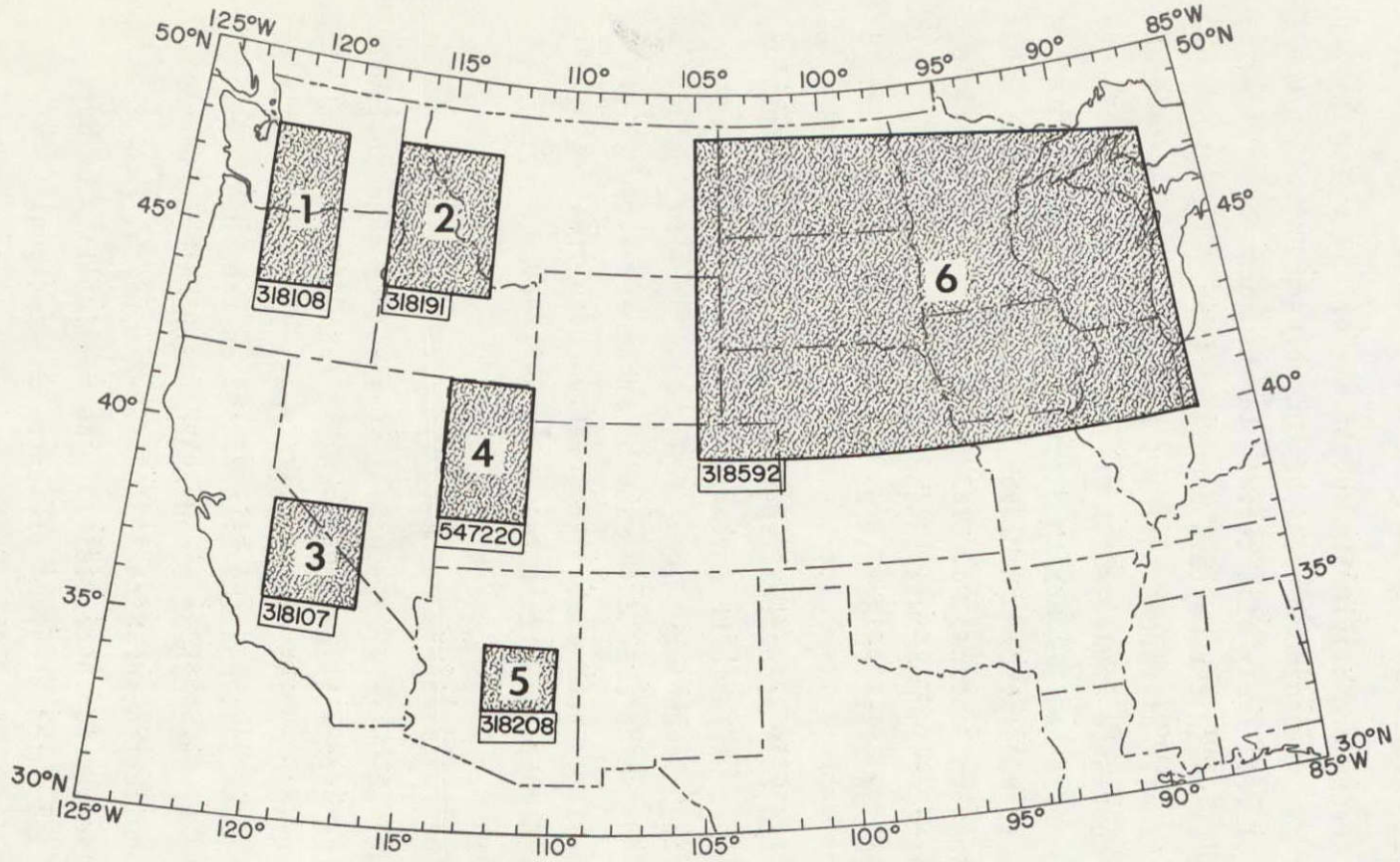

Figure 2-1 Map showing originally specified test site areas: (1) Cascades, (2) Upper Columbia Basin, (3) Sierra Nevada - Walker Lake, (4) Wasatch Range in Utah, (5) central Arizona and (6) Midwest.

2.2.1 Site 318107: Sierra Nevada

The portion of the Sierra Nevada test site covered by EREP pass 3 (3 June 1973) and Pass 98 (1 February 1974) is shown in Figure 2-2. In early June, snow existed in the Sierras and the White Mountains; at the time of the Skylab pass, cumulus clouds covered a part of the area, especially over the Sierras west of Mono Lake and Lake Tahoe. On Pass 98, most of the northern portion was obscured by clouds, whereas the area between Walker and Mono Lakes was partially cloud covered; at that time, snow existed on some of the smaller ridges as well as the high mountains.

This site is an area of fault-block mountains, which can rise to elevations of 4,000 meters in a horizontal distance of only a few miles. Due to the more arid climate on the eastern side of the Sierras, very sparse desert type vegetation exists at the lower elevations, whereas the higher elevations support some pine and pine-douglas fir forest types. Numerous intermittent streams as well as some lakes and rivers dissect the landscape in this site.

2.2.2 Site 547220: Wasatch Range

Data were collected on EREP Pass 5 (5 June) over the Wasatch area in central Utah, including the Wasatch Plateau, San Pitch Mountains, and Mt. Nebo Range (Figure 2-3). On this date, snow remained on the higher elevations, and the area was completely cloud-free at the time of the Skylab pass. In this mountain area, elevations range from 1550 meters in the valleys, to over 3190 meters on the mountain ridges. Urban development consists of a few highways and railroads with a few scattered towns. Major forest types in the area include fir-spruce on the higher elevations, hardwoods at mid-elevations, and pinyon-juniper on the flanks of the ridges.

2.2.3 Site 318208: Central Arizona

The central Arizona mountains contain the Salt-Verde Watershed, a drainage area from which most of the surface runoff for Arizona is derived. The area was cloud-free when overflown by Skylab on Pass 83 (14 January). A substantial snowpack existed in the mountains at that time.

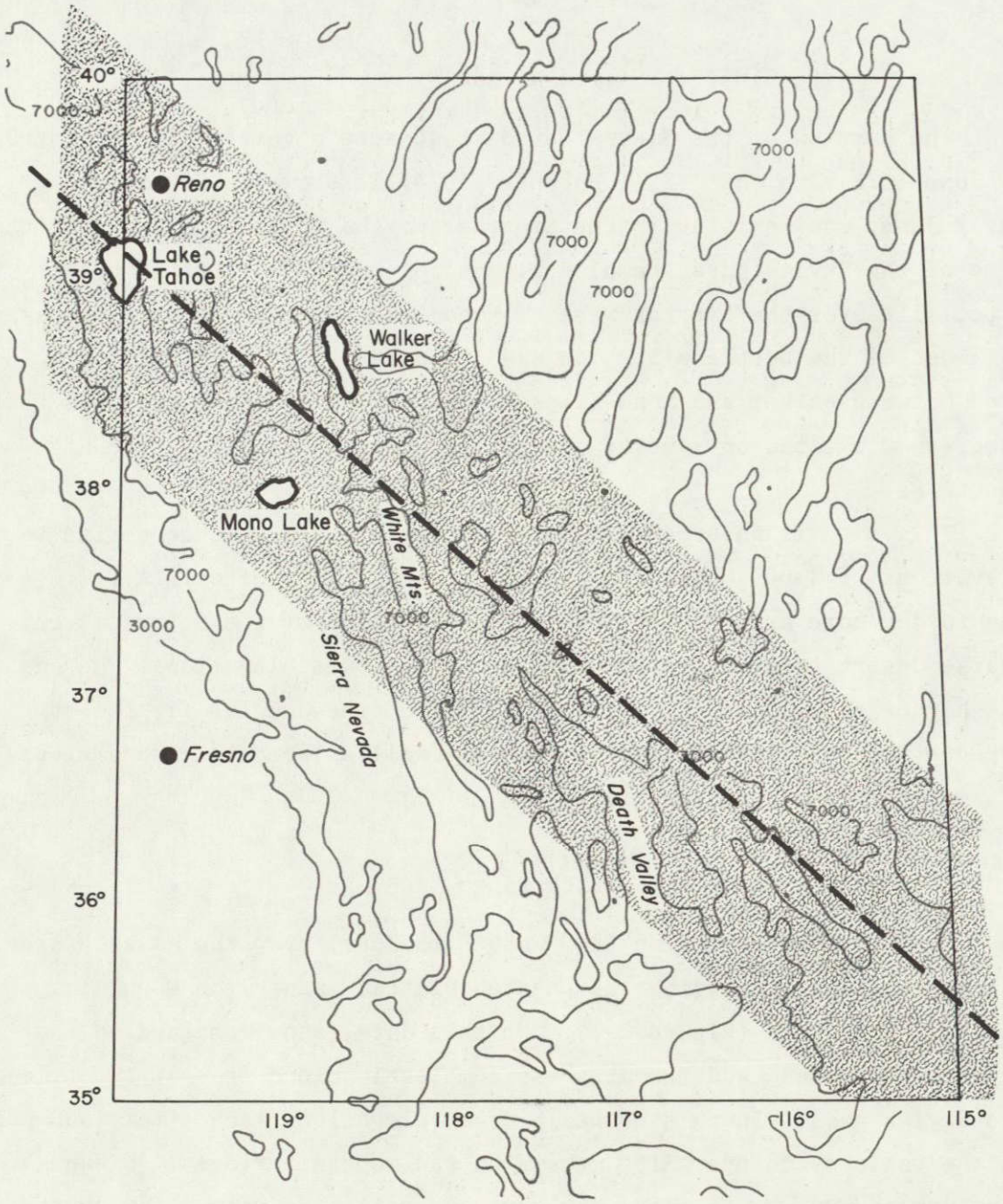

Figure 2-2 Diagram showing ground track of EREP passes 3 on 3 June 1973 and 98 on 1 February 1974 over the Sierra Nevada - Walker Lake area (Test Site 318107). (Pass 98 was offset by 1° to the northeast of Pass 3.) Shaded portion indicates area of coverage for the S190A photography. Contours for 900 m (3,000 ft.) and 2100 m (7,000 ft.) are indicated.

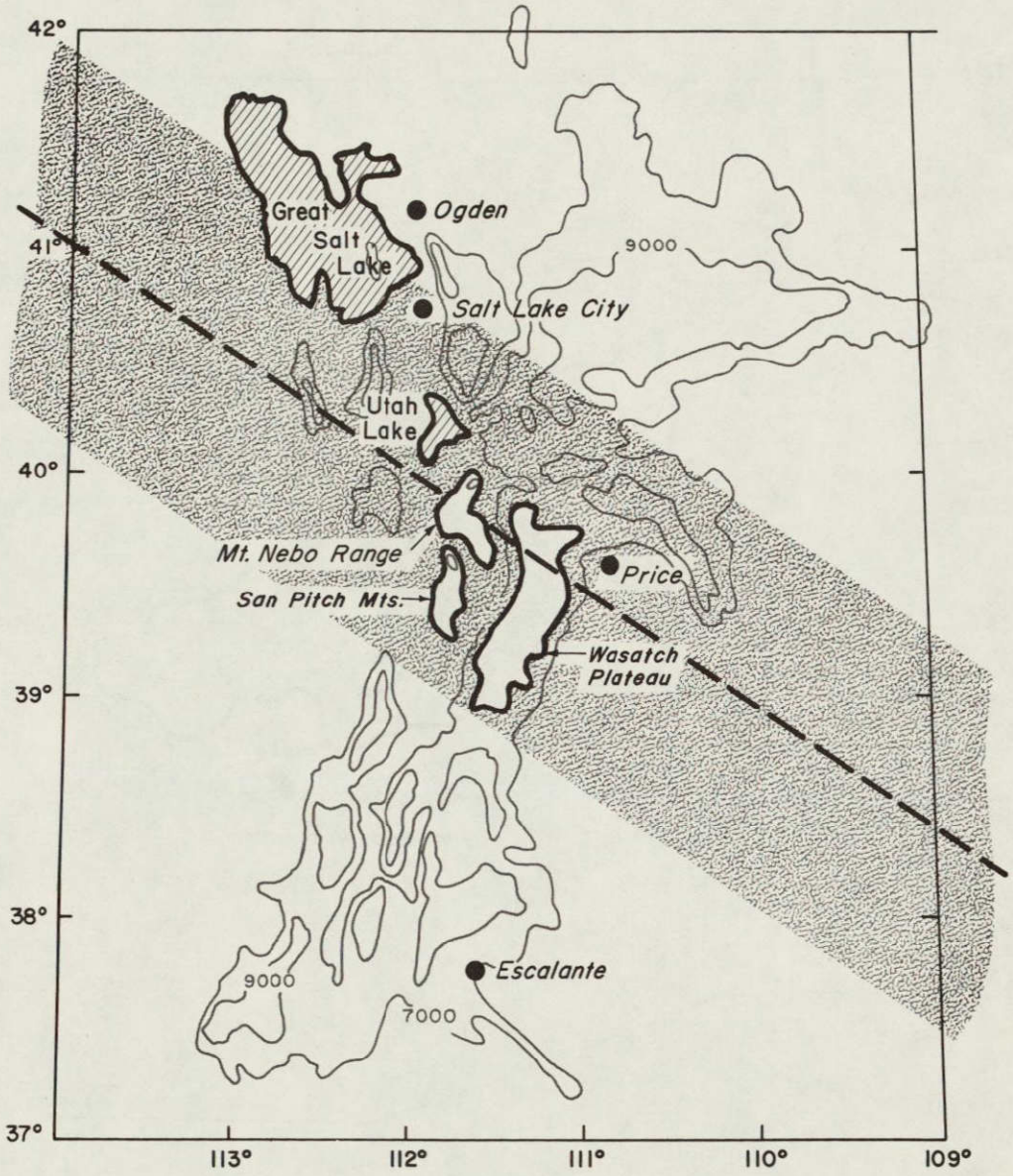

Figure 2-3 Diagram showing ground track of EREP Pass 5 over the central Utah area on 5 June 1973 (Test Site 547220). Shaded portion indicates area of coverage for the S190A photography. Contours for 2100 m (7,000 ft.) and 2700 m (9,000 ft.) are indicated.

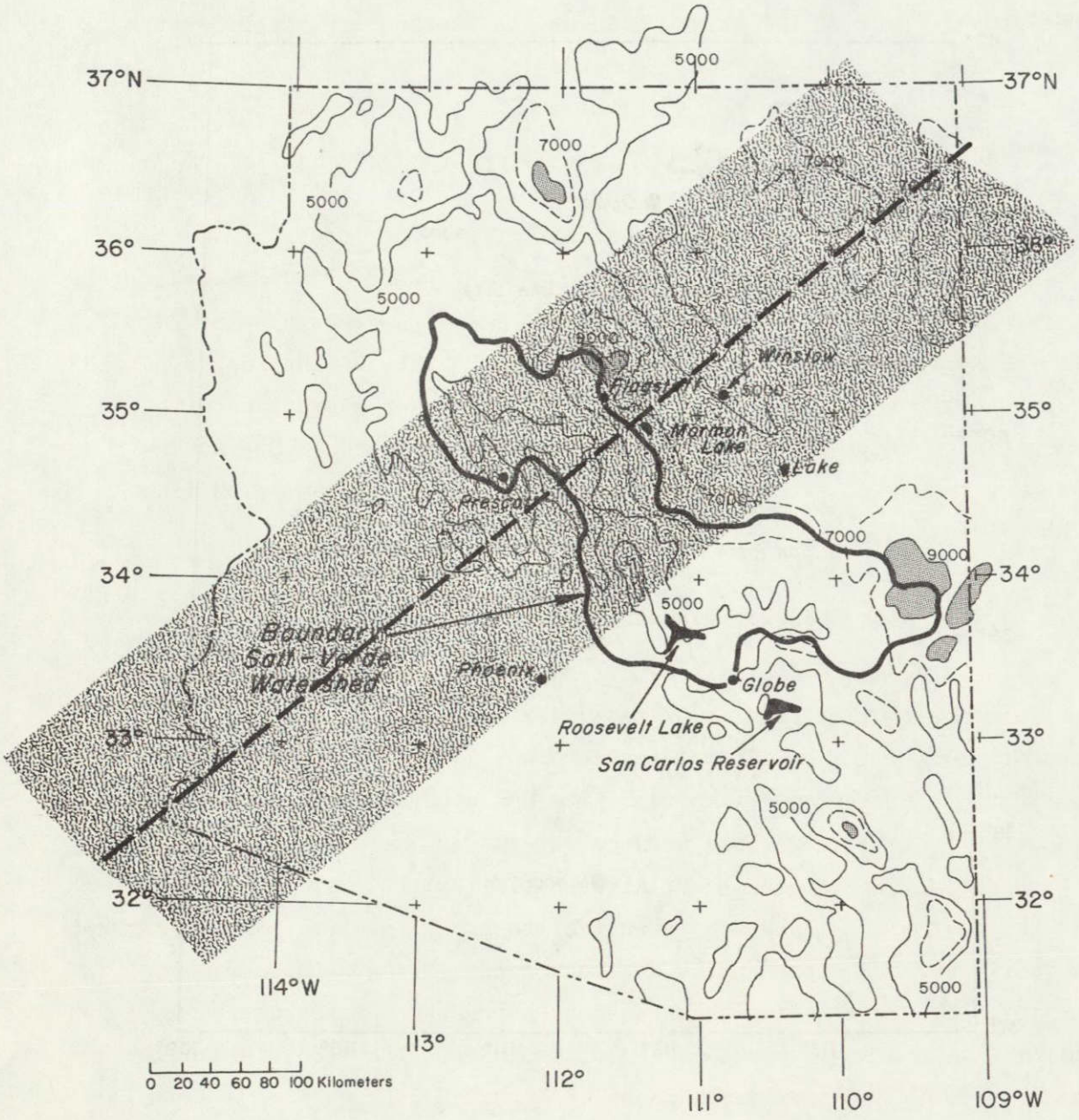

Figure 2-4 Diagram showing ground track of EREP pass 83 over central Arizona (Test Site 318208) on 14 January 1974. Shaded portion indicates area of coverage for the S190A photography. Contours for 1500 m (5,000 ft.), 2100 m (7,000 ft.) and 2700 m (9,000 ft.) are indicated.

751331 7509

The ground-track of the Skylab pass and the boundaries of the Salt-Verde Watershed are shown in Figure 2-4.

Much of the test-site is of volcanic origin with the Central Mountains rising to elevations of 2,000-2,500 meters. Virtually all of the Salt-Verde Watershed is located in the Coconino National Forest where ponderosa pine and pinyon-juniper are the dominant forest types. To the east and southeast and also to the southwest of Mormon Lake, there are broad areas of lower elevation (900-1600 meters) which are, for the most part, either non-forested or chaparral. The rugged topography has confined urban development to the lower elevations with Flagstaff being the largest city in the test site area. One major highway traverses the mountains and several power transmission line swaths cross the area.

2.2.4 Site 318592: Midwest

The Midwest test site area offers an opportunity to examine the reflectance characteristics of snowcover over fairly uniform, level terrain mostly in agricultural production. Forested areas exist in the northeast section of the test site and along the river basins in the area. Elevations range between 300 and 600 meters. Being part of the Upper Mississippi-Missouri River Basin, numerous streams are evident in the test site. The area is subject to heavy snowfall, which assumes a fairly uniform distribution due to a general lack of topographic relief. This test site was crossed by three EREP passes on the SL-4 mission; the ground tracks of two of the passes (Pass 83, 14 January; and Pass 89, 24 January) are shown in Figure 2-5.

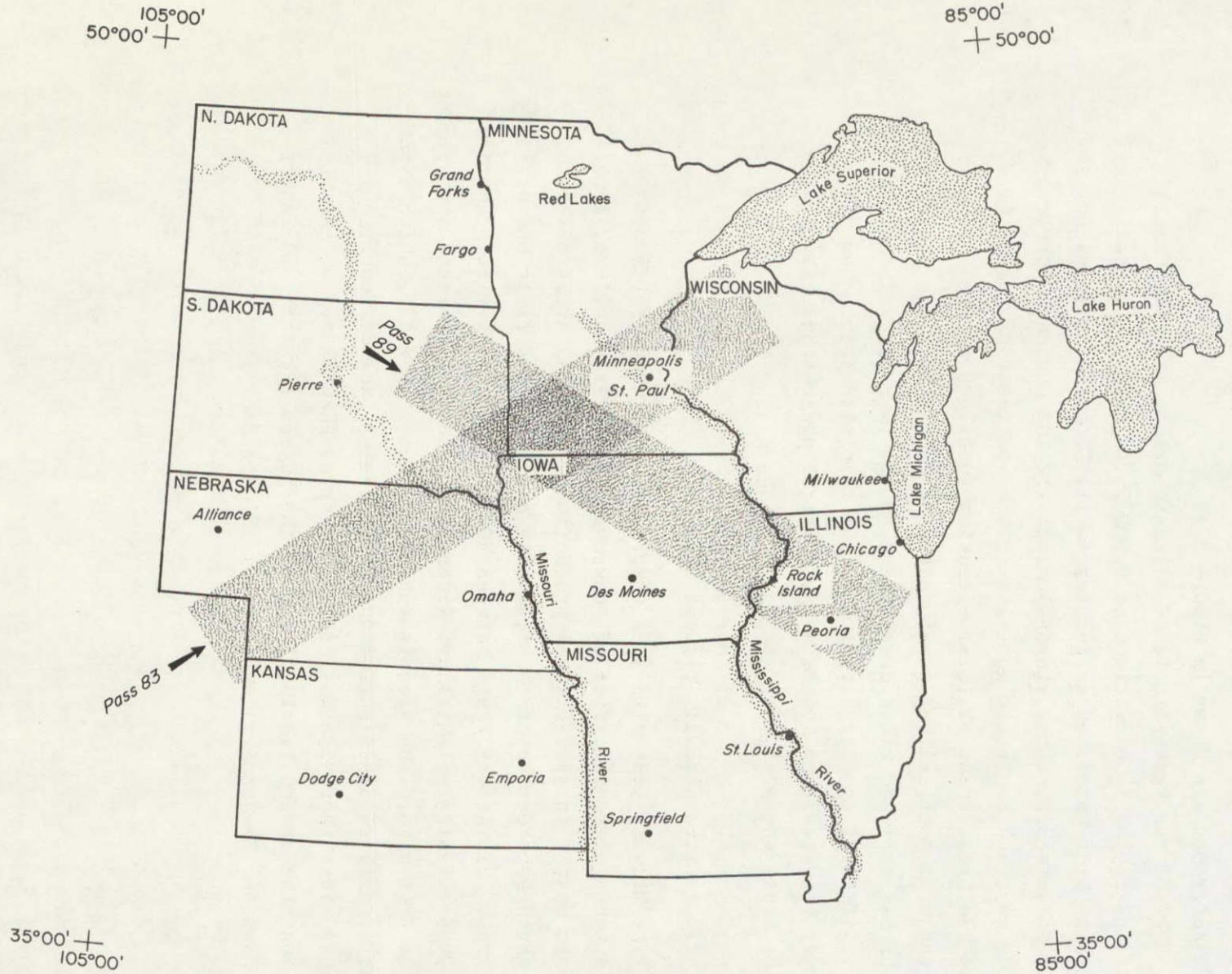

Figure 2-5 Diagram showing ground track of EREP passes 83 on 14 January 1974 and 89 on 24 January 1974 over the Midwest (Test Site 318592). Shaded portions indicate area of coverage for the S190A photography.

3. DATA SAMPLE

3.1 Skylab EREP Data

As stated in the previous section, Skylab EREP data were collected over each of the specified test site areas, except Site 318191. Data were available for analysis from three passes on the SL-2 mission in June 1973 and four passes on the SL-4 mission in January-February 1974. It is of interest that data for Site 318107 were collected on one of the first EREP passes (Pass 3) and then on the final EREP pass of the Skylab mission (Pass 98) on 1 February 1974. The types of data products available for each test site are listed in Table 3-1.

As can be seen in Table 3-1, a variety of EREP data were available for analysis. The S190A multispectral camera acquired black and white photography in both the visible and near-infrared bands as well as color and color-infrared transparencies; the S190B Earth Terrain Camera acquired high resolution color or color-infrared photography. Both of these photographic products provided an excellent source of ground truth to aid in interpretation of the data from the other EREP sensors.

Data products such as the S190A and S190B photographs and the S192 screening film were available for the complete segments of the Skylab ground tracks crossing the specified test site areas. Other data products, such as the S192 digital tapes, were acquired for only limited segments over specific target sites; the specific segments were selected from review of the screening film.

The particular sensor systems are briefly described in the later sections in which the data analysis is discussed. Complete descriptions of the Skylab EREP sensors and data products are given in publications such as "The Earth Resources Production Processing Requirements for EREP Electronic Sensors" (Aerospace and Defense Systems Operations, 1973); the Skylab Program EREP Investigators' Information Book" (Mission Requirements and Operations Team, 1973); and the "Skylab Earth Resources Data Catalog" (NASA, 1974). Sensor Performance Reports were also prepared for each sensor of the Skylab Earth Resources Experiment Package, and are available from NASA/JSC (Earth Resources Program Office).

TABLE 3-1

SKYLAB DATA SAMPLE

Test Site	Date	EREP Pass	SL Mission	Photographic Products			Computer Compatible Tape Products (CCT)			
				S190A	S190B	S192	S191	S192	S193	S194
318107 Sierra Nevada California	3 Jun 73	3	2	X		X	X		X	X
547220 Wasatch Range Utah	5 Jun 73	5	2	X	X	X		X		
318108 Cascades	11 Jun 73	8	2	X					X	X
318208 Central Arizona Mountains	14 Jan 74	83	4	X	X	X		X		X
318592 Midwest	14 Jan 74	83	4	X	X	X				X
318592 Midwest	24 Jan 74	89	4	X	X	X		X		X
318592 Midwest	25 Jan 74	90	4	X		X				X
318107 Sierra Nevada California	1 Feb 74	98	4	X	X	X		X		X
318191 Upper Columbia Basin	- No data collected for this test site due to cloud interference									

3.2 Correlative Data

Correlative data consisted of imagery from the Landsat-1 satellite, aircraft photography, aerial survey snow charts, standard snow reports, and standard meteorological observations. An aircraft underflight was flown for Test Site 318208 (central Arizona) by NASA's Earth Resources Aircraft Program (ERAP) on 15 January 1974 to correlate with EREP Pass 83. A high-altitude data pass (60,000 feet) by a WB57F aircraft equipped with an RC-8 camera provided high quality color photography (SO-397 film) at a scale of 1:120,000. High altitude aircraft color photography was also obtained for portions of the Sierra Nevada test site on 28 January 1974 during a series of three data flights by the WB57F aircraft (Mission 260). However, the ground tracks of these flights covered the southern portion of the Sierras, whereas the Skylab pass on 1 February crossed the northeastern portion of the test site. In addition to photography, thermal infrared imagery was collected on the aircraft flights; since the Skylab data analysis was concentrated on snow reflectance in the near-infrared, the aircraft thermal infrared data were not used.

An aerial survey was flown over the Salt-Verde Watershed in central Arizona on 15 January by the Salt River Project Office; the resulting snow chart provided an excellent source of information on snow extent and estimated snow depths. The snow reports and other meteorological data were taken from sources such as the Climatological Data Books published by the Environmental Data Service of the National Oceanic and Atmospheric Administration.

3.3 Data Selected for Analysis

In the experiment plan the S190A and S190B photographs were to be used primarily to map snowcover extent to provide ground truth information in support of the analysis of data from the other EREP sensors. For each EREP pass, therefore, the photography was examined first to identify the snowcover and to select the segments of the pass that would be most appropriate for further data analysis. Additionally, analysis was performed to assess the utility of the improved camera resolutions of the S190A and S190B for snow mapping as compared to aircraft and other spacecraft observations.

The major effort in the investigation was devoted to the analysis of the S192 Multispectral Scanner data. The S192 provided for the first time, the opportunity to examine the reflectance characteristics of snow from space in several spectral bands in both the visible and near-infrared. Moreover, the high resolution of this sensor (approximately 80 meters) permitted the reflectances of relatively small area targets on the ground to be examined. In the analysis of the S192 measurements, both the film products and the computer compatible tapes were used.

Only one sample of data from the S193 Radiometer-Scatterometer (RADSCAT) was obtained. Data from the S194 L-Band Radiometer were available for each EREP pass. The digital values for the S193 were analyzed for the one pass, and the digital values for the S194 were analyzed for three passes. The effort devoted to the analysis of the microwave data was considerably less than that to the S192 data, principally because the spatial resolutions of the sensors were not sufficient to permit correlation of the measured brightness temperatures with the snowcover. This was especially true with the S194 data, where only large scale geographic features could be identified.

A limited amount of data from the S191 Spectrometer was also obtained for a segment of one EREP pass, but these data were not used in the study. The original intent was to use the S191 measurements to examine the influence of the atmosphere on the measurements from the various sensor systems. However, in a separate Skylab/EREP investigation being conducted at ERT (Investigation EPN 439), a thorough study of the atmospheric attenuation effects is being carried out. Since the preliminary results of that study (Chang and Isaacs, 1975) indicate that the effects of the atmosphere on the measurement of snow reflectance are not significant, it was decided that to undertake the rather tedious task of processing S191 data would not be necessary.

4. ANALYSIS OF S190A AND S190B PHOTOGRAPHY

4.1 Data Format

The EREP S190A (Multispectral Photographic Camera) is a unit containing six high precision lenses used to cover a particular spectral region in both black and white and color. The S190A covers an area on the ground of 163 by 163 km at a resolution of 30-70 meters. The design wavelength and film types are shown in Table 4-1.

TABLE 4-1

S190A DESIGN WAVELENGTHS AND FILM TYPES

Station no.	Design bandwidth, μm	Film, 4-mil base	Estimated Ground Resolution (meters)
1	0.7 to 0.8	IR aerographic B&W, type EK 2424	73 - 79
2	.8 to .9	IR aerographic B&W, type EK 2424	73 - 79
3	.5 to .88	Aerochrome IR color, type EK 2443	73 - 79
4	.4 to .7	Aerial color (high-resolution), type SO-356	40 - 46
5	.6 to .7	PAN-X aerial B&W, type SO-022	30 - 38
6	.5 to .6	PAN-X aerial B&W, type SO-022	40 - 46

The S190B Earth Terrain Camera is a single camera assembly used to obtain higher resolution photographs than the S190A: The field-of-view covers an area on the ground of 109 by 109 km at a resolution of 15-30 meters. Various types of film including black and white, aerial color and color infrared were used in the S190B camera. Complete descriptions of these photographic sensors are given in the NASA publications referenced in Section 3.1.

4.2 Summary of Results of Preliminary Analysis

In the experiment plan the S190A and S190B photography were to be used primarily to map snowcover extent to provide ground truth information in support of the analysis of data from the other EREP sensors, such as the S192 Multispectral Scanner. In addition to using the photography for this purpose, analysis was performed to assess the utility of

the improved camera resolution of the S190A and S190B for snow mapping as compared to other spacecraft systems such as Landsat. The results of earlier studies (Barnes, Bowley, and Simmes, 1974; Bowley and Barnes, 1975) have shown that Landsat-1 imagery has substantial practical application to snow mapping.

Much of the analysis of photographic data was carried out earlier in the study using photography collected on the SL-2 mission over three test site areas in the western United States in which mountain snowcover existed. Because of the late spring season, the snow was confined to the higher elevation terrain. The results of the analysis of the SL-2 data, which were reported in detail in an Interim Report (Barnes, Bowley, and Smallwood, 1974), are summarized in the following paragraphs.

Of the four black and white S190A camera stations, snowcover is best defined in the two visible spectral bands, due in part to their better resolution. The overall extent of the snow can be mapped more precisely and the snow within shadow areas is better defined in the visible bands. In some instances, however, variations in reflectance within snowcovered areas are observed in the near-infrared bands but not the visible; these variations may be associated with forest effects or even snow depth.

Of the two S190A color products, the aerial color photography is the better. In fact, because of the contrast in color between snow and snow-free terrain and the better resolution, this product is concluded to be the best overall of the six camera stations for detecting and mapping snow. Excellent definition between snow and bare rock within shadow areas is observed in the aerial color photographs. In the color-infrared product, the edges of the snowpack tend to have a bluish tone similar to that of the adjacent terrain, and, thus, are not precisely defined; the bluish tone may be the result of patchy snow mixed with forest.

The overlapping S190A frames permit stereo viewing, which aids in distinguishing clouds from the underlying snow. Over the highest terrain, however, the distinction is more difficult because of the smaller difference in the elevation of the clouds and the terrain. Therefore, subjective interpretive keys, such as those developed for analysis of Landsat data, must generally be used to distinguish snow from clouds.

Because of the greater spatial resolution of the S190B Earth Terrain Camera, areal snow extent can be mapped in greater detail than from the S190A photographs. In the one test site area for which S190B photography was available, small areas of snow lying along narrow ridges could be detected that were not observed even in the S190A aerial color film. As was true with the S190A data, the S190B aerial color product was better than a black and white print (processed from the color transparency) because of the contrast in color tone as well as the contrast in reflectance.

The snow line elevation measured from the S190A and S190B photographs is reasonable compared to the meager ground truth data available. Comparisons between the areal snow extent mapped from the S190A black and white visible band photographs and that mapped from Landsat-1 imagery indicate that the snow line can be defined in greater detail from the Skylab product. Moreover, the definition of snow in the S190A aerial color photographs is considerably better than the definition in the Landsat imagery.

Previous investigations have shown that snow can be mapped in more detail from Landsat than from aerial surveys and that the snow line elevation can be measured from Landsat to an accuracy of about 60 m. Thus, although it was not possible to determine the areal snow extent in a complete river basin, the greater detail in the S190A photographs gives every indication that the snow line elevation can be mapped to an accuracy of better than 60 meters. Therefore, based on the results of the analysis of the SL-2 data sample, the overall conclusion is that areal snowcover extent can be mapped more accurately from the S190A and S190B photography than from any other spacecraft system.

4.3 Analysis Procedures

4.3.1 Processing of Imagery

Further analysis of the S190A and S190B photography from the SL-4 mission was performed when these data were received later in the study period. For selected frames enlarged prints were processed from the 70 mm negatives. The enlargements were made to a scale of slightly larger than 1:500,000, which was found to be a useful scale with regard to the mapping of detailed snowcover patterns. Prints were made for

each of the S190A black and white spectral bands. For the two S190A color products, black and white enlargements were also made; subsequently color prints were processed for selected frames. Enlarged black and white prints of similar scale were processed from the S190B color film; as with the S190A color film, color prints were then processed for selected frames.

4.3.2 Use of Optical Mapping Devices

In the analysis of the photographs use was made of two optical mapping devices. One device is a Zoom Transfer Scope, a device which allows optical matching of two different scales, as well as rectification of slight photographic distortion. In using the ZTS, the image (either a print or a transparency) is superimposed optically onto a base map. Through adjustment of the image projection size and through stretching of the image along either axis, the original image is rectified to fit the exact scale of the base map. Once these procedures have been completed it is possible to map snow extent from the image directly onto a base map of desired scale.

A second optical device, a Variscan rear projection viewer, was also found to be useful for the task of mapping snow boundaries and determining estimated snow line altitudes. The procedure was first to tape a clear, acetate overlay, with landmarks taken from a 1:250,000 scale topographic map, to the viewing screen of the Variscan. A 70 mm S190A transparency was then projected onto the viewing screen. Proper scale matching between the transparency and the overlay was not possible using the original lenses in the Variscan, so an 80-200 mm zoom lens was substituted in one of the lens stations. Final adjustments to image size were made and the desired scale was achieved. The snow boundaries were traced onto the overlay using a technical drawing pen, and the resultant product was a line drawing of the snow extent at a scale of 1:250,000. The overlay was removed from the viewing screen and placed over the appropriate topographic map where determinations of the snow line altitude could be made.

The advantages to using the Variscan in such a manner are threefold: first, the time it takes to map the snow boundaries and trans-

fer the information to a base map is reduced significantly; second, the increased scale of the Variscan image (1:250,000) allows a more accurate interpretation of the snow boundary; and finally, the 70 mm S190A aerial color transparencies can be utilized with no need for the higher priced color enlargements.

4.4 Results of Analysis of Photography from the SL-4 Mission

4.4.1 Analysis of Forest Effects and Snowline Elevation in Central Arizona Test Site Area

Both S190A and S190B photography from EREP Pass 83, on 14 January, were analyzed for the central Arizona test site area (a map of the test site area, showing the boundaries of the Salt-Verde Watershed and other geographic features, is given in Figure 2-4). The S190A photograph of the area is given in Figure 4-1. An aerial snow survey chart, compiled on 15 January indicates a rather uniform snowcover in the area, ranging from 41-76 cm (16-30 inches). Whereas the measured snowcover appears uniform throughout the watershed, examination of the S190A and S190B photography shows that the reflectance within the area of snowcover varies significantly.

Using the techniques discussed above, a 70 mm S190A aerial color transparency was analyzed with the aid of the Variscan, and a detailed overlay of snow boundaries and the boundaries of reflectance variations within the snowcovered area was constructed. When the overlay was applied to the topographic map, as shown in Figure 4-2, the correlation between areas of forest cover on the map and areas of low reflectance on the overlay is obvious. This comparison also indicates that non-forested areas are slightly more extensive on the photography than indicated on the topographic map; snow enhancement, therefore, can aid in the updating of maps which indicate forested vs. non-forested land utilization.

The feasibility of using the Skylab S190B photography to monitor certain silvicultural practices was also examined. Since the reflectance of snowcover in forested areas is related to tree density and possibly tree type, certain cutting methods such as strip cutting, clear cutting, and selective cutting should have varying effects on the reflectance of the snowcover. The Coconino National Forest in central Arizona (Figure 4-2) is an ideal test area for such an investigation

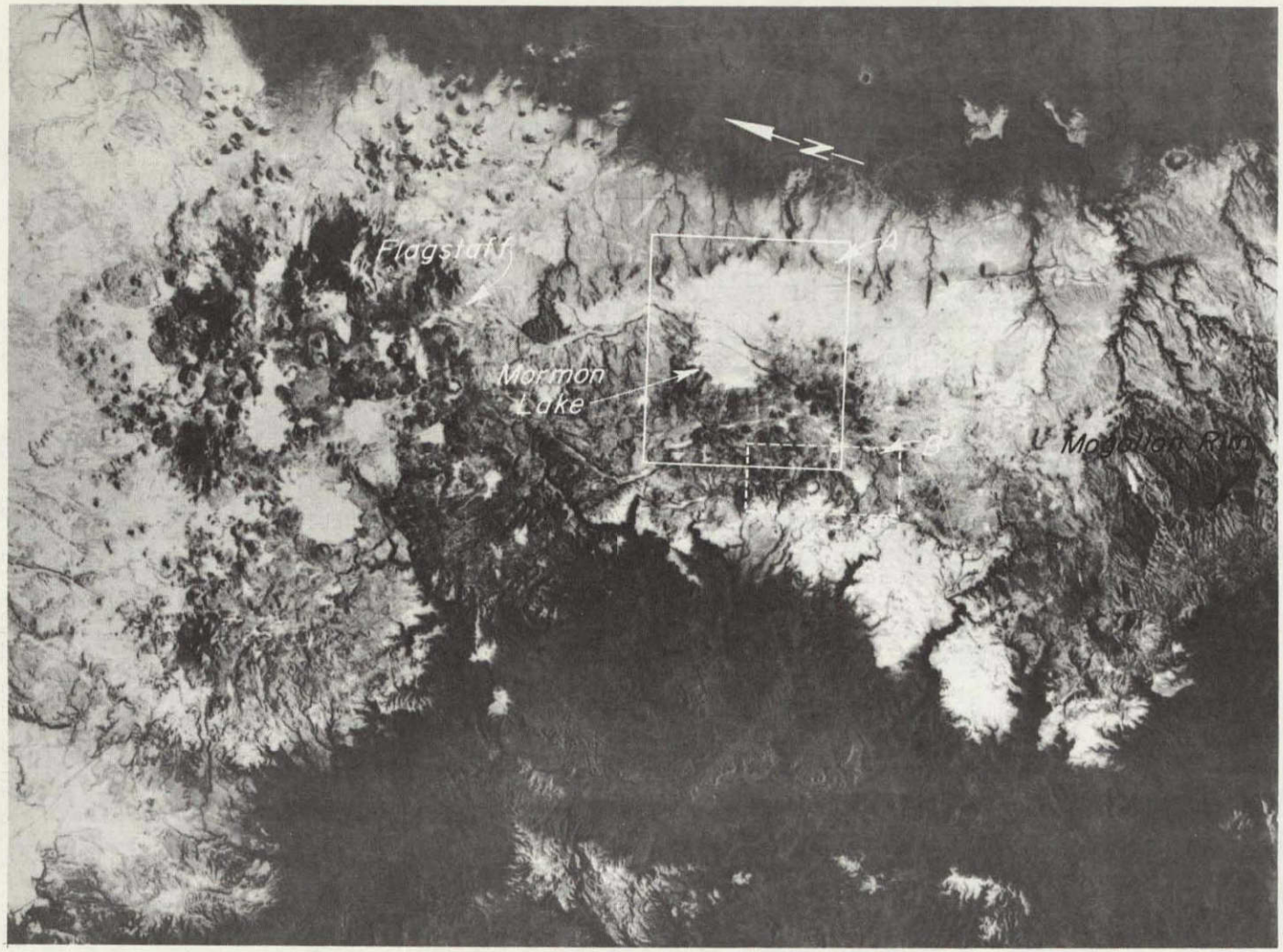

Figure 4-1 S190A Camera Station 6 (0.5 - 0.6 μm) photograph viewing Central Arizona on 14 January 1974. Outlined area (A) represents area shown in Figures 4-6, 4-7, 4-8. (B) represents area shown in Figure 4-3.

Figure 4-2 Portion of USGS Topographic Map showing central Arizona. Black lines indicate boundaries of areas with differing reflectances as mapped from S190B photograph (H, M and L indicate high, medium and low reflectance, respectively). Blue line indicates snow boundary as depicted on aerial survey snow chart.

since variation in species (ponderosa pine and pinyon juniper) and silviculture exist, associated with the Beaver Creek Experimental Watersheds. The general objective of the Beaver Creek Project is to evaluate land management measures designed to increase water yields (Brown, et al, 1974; Clary, et al, 1974).

Three watersheds, designated as Watershed Test Sites 9, 12, and 14, were selected to examine the effect of cutting methods on the snow reflectance. Figure 4-3 is a black and white enlargement of an S190B color-infrared photograph showing the areas covered by the three watersheds. Descriptive material on the Beaver Creek Project states that 33 percent of Watershed 9 was clearcut in uniform strips 20 meters wide with spacing between cut strips of 40 meters; Watershed 14 was cleared in irregular cut strips averaging 20 meters wide with the intervening 40 meter wide strips thinned out; and Watershed 12 was totally clearcut and essentially removed from timber production. The S190B photograph demonstrates that although the snow depth in this area is fairly uniform, the reflectance in each watershed is different. In Watersheds 9 and 14, the cut strips have a high reflectance whereas the uncut strips have a lower reflectance; in Watershed 12, where there is no tree canopy to obscure the snowcover, the reflectance is high; in Watershed 14 the tree density has been decreased by thinning, resulting in a somewhat higher reflectance than for unthinned areas.

Using the overlay prepared on the Variscan viewer in conjunction with the topographic map (Figure 4-2), it was also possible to determine the mean snowline elevation. The elevation was determined at many data points along the slopes to the west and southwest of Mormon Lake from Sycamore Canyon to the western extent of the Mogollon Rim. These data points were then averaged and a mean snowline elevation of 1750 meters (5,775 feet) was determined for the central Arizona mountains. The snowline as depicted on the aerial survey snow chart compiled a day after the Skylab pass is also plotted in Figure 4-2. A comparison between the snowline positions mapped from the S190B photograph and by the aerial observer demonstrates the greater detail and positional accuracy of the Skylab data. The aerial survey snowline is considerably less detailed, and the position of the snowline does not fit the topography as closely as does the Skylab snowline.

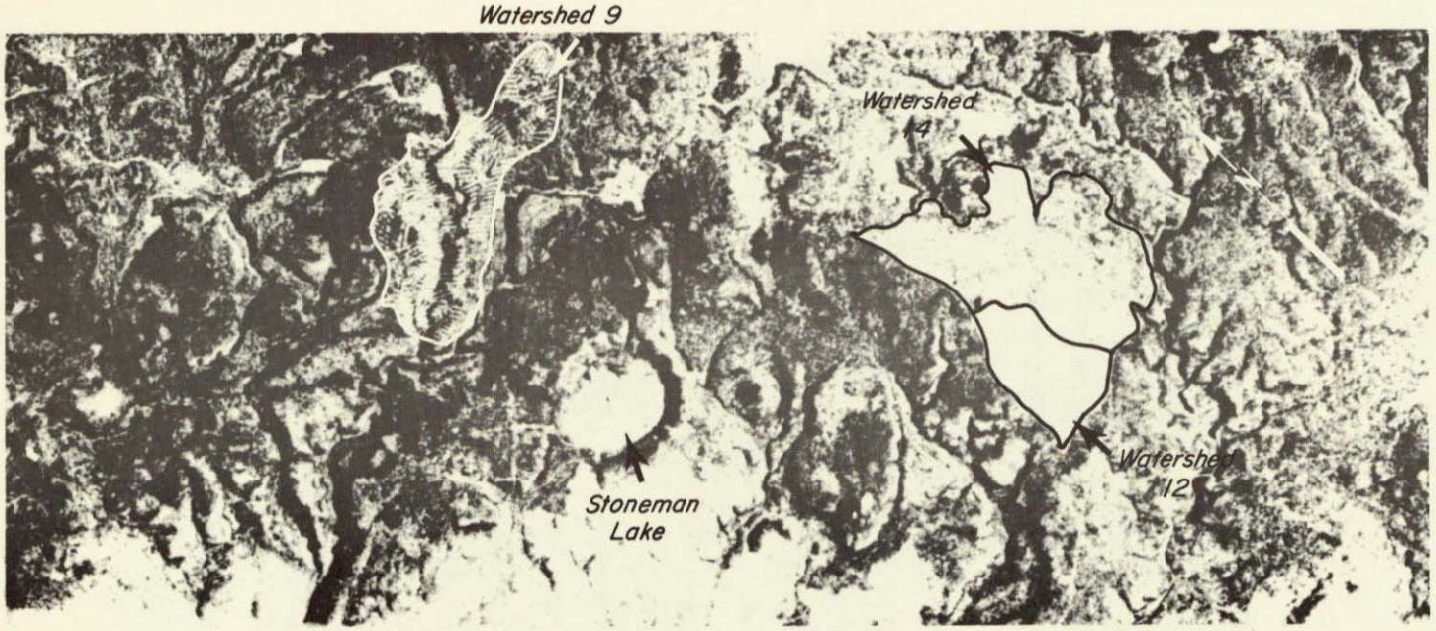

Figure 4-3 Enlarged S190B photograph showing variation in snowcover reflectance in each of three experimental watersheds in central Arizona (Stoneman Lake is also indicated).

Figure 4-4 S190A Camera Station 4 (aerial color; 0.4 - 0.7 μm) photograph viewing the Central Arizona test site.

Figure 4-5 Skylab-4 S190B (color-infrared; 0.5 - 0.88 μm) photograph viewing the central Arizona test site.

4.4.2 Comparison Between S190A and S190B Color Photographic Products for the Central Arizona Test Site Area

A comparitive analysis was performed using the S190A aerial-color product and the S190B color-infrared product (in earlier analyses, the S190A aerial color and color-infrared products were compared as discussed in Section 4.2). The respective color photographs are shown in Figures 4-4 and 4-5. As was found in the preliminary analysis of the S190A color-infrared photographs, there is a tendency in the S190B color-infrared for areas of patchy snow along the limits of the snow/no snow boundary to diffuse into the bluish background tone; however, this tendency is greatly minimized due to the increased resolution of the S190B sensor. Also, whereas in the S190A (aerial color) photography many snowcovered areas with a sparse tree density appear to have the same reflectance as snowcovered non-forested areas, it is possible to distinguish between these two areas using the S190B photography. In the area just north of Stoneman Lake, for example, the parallel cutting swaths of a clear-cutting operation in the Ponderosa Pine forests are readily discernible as dark and light strips on the S190B transparency; these strips merge into a single area of lighter tone in the S190A image.

The comparison between Figures 4-4 and 4-5 also reveals that the ice cover on many of the lakes has a lower reflectance than the surrounding snowcover in the S190B imagery; this difference is much less on the S190A aerial color product. Furthermore, the increased resolution of the S190B color-infrared photograph does give a more accurate indication of the patchy snow along the valley slopes, and more detail is observed in forested areas where the reflectance of the snowcover is greatly reduced.

4.4.3 Comparison Between Skylab Photography, Aircraft Photography, and Landsat Imagery for Central Arizona Test Site Area

An aircraft photograph, a Skylab S190B photograph, and a Landsat-1 image, all covering the same area, are shown in Figures 4-6, 4-7, and 4-8, respectively. To facilitate comparison of these products from sensors with different spatial resolutions, each was processed to a scale of approximately 1:120,000 (the original scale of the aircraft photograph; see Section 3.2). The Skylab and aircraft data are on 14 and 15 January, whereas the Landsat-1 image is several days later, on 27 January.

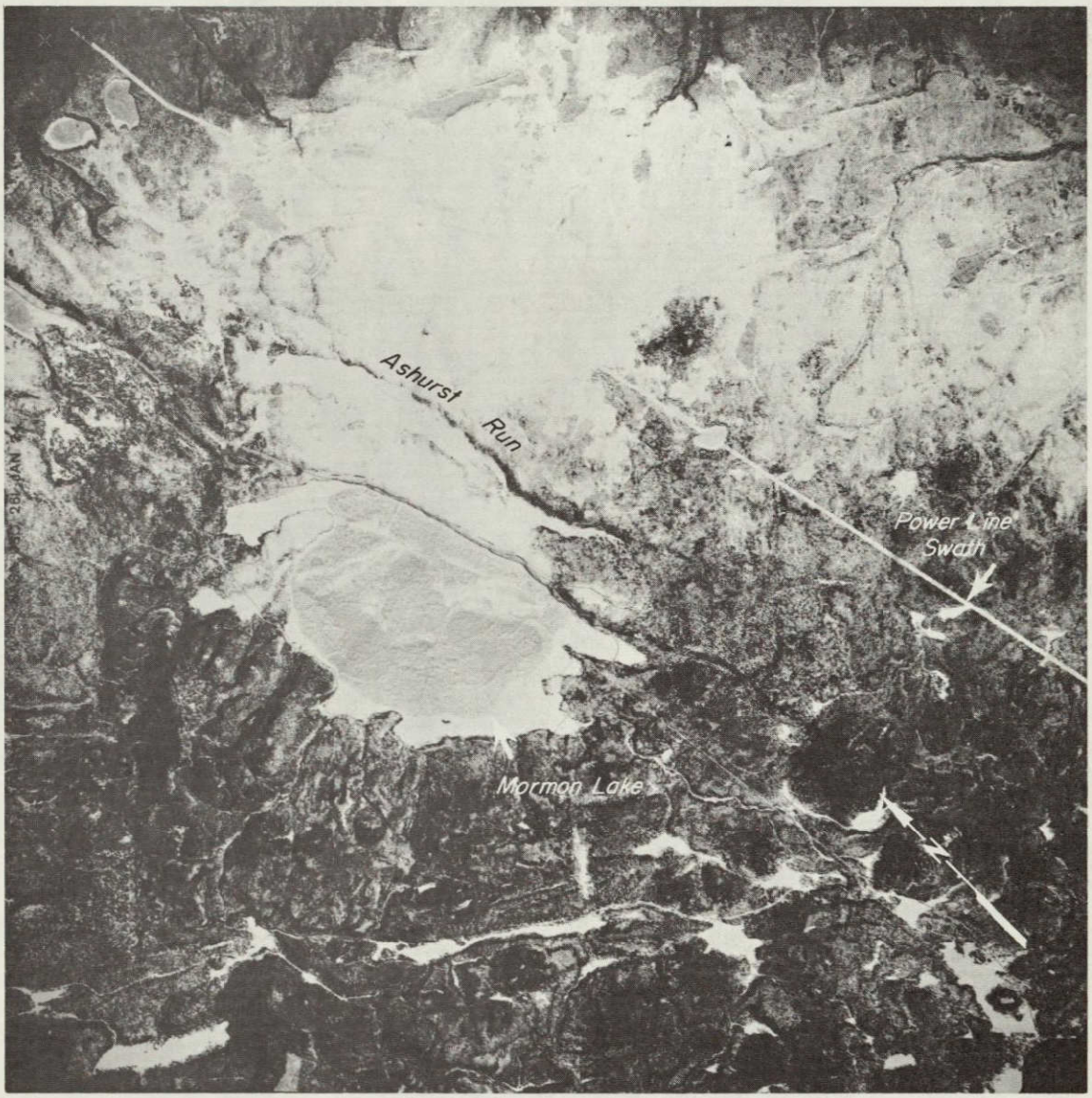

Figure 4-6 NASA aircraft photograph taken on 15 January 1974 (scale 1:120,000) showing portion of central Arizona test site area. Mormon Lake, Ashurst Run, and power transmission line swath are indicated.

Figure 4-7 Enlargement of S190B photograph to same scale as the aircraft photograph shown in previous figure.

Figure 4-8 Enlargement of Landsat image to same scale as the aircraft photograph shown in Figure 4-6.

Although the Landsat image reveals a greater overall snow extent within the Salt-Verde Watershed to the south of the Mogollon Rim and north of the watershed toward the desert region, only slight differences are observed within the area shown in the aircraft photograph (Figure 4-6). The widespread snowfall of 5-10 cm that occurred early on the 27th resulted in only a slight southward progression of the snow extent into forested terrain located south of the higher reflecting flat-topped mesas previously observed as the southern snow extent.

The aircraft photograph is by far the most detailed product, but the other two products (especially the S190B) could also be used to extract a large amount of information. The Landsat-1 image has been enlarged 24X and it is still possible to map fairly accurately the snowcover in open, non-forested areas. Some snowcovered, forested areas are also discernible; however, the accuracy of measurements of snowcover in these areas would be low.

The amount of detail afforded by the S190B photograph is very nearly the same as that of the aircraft photograph. The S190B print has been enlarged 7.5X, and it is possible to map snowcover in forested and non-forested areas; patchy snow, the ice on Mormon Lake, and even the alternating dark and light strips associated with silvicultural practices are discernible in the lower right-hand corner of the photograph (see Section 4.4.1). Since the photo was generated from a black and white negative made from a color transparency, additional detail was sacrificed. It is highly possible that an enlargement of this size made from a high-definition aerial black and white film type, such as the EK 3414 utilized in the S190B sensor on some passes, would produce a product of essentially the same quality as the aircraft photography.

4.4.4 Midwest Test Site

Analysis of snowcover in the Midwest afforded an opportunity to determine if there were any significant differences in the appearance or behavior of snowcover in flat terrain as compared to mountainous terrain. Skylab coverage was available for three passes over the Midwest; the area of intersection for two of these passes was selected for analysis. EREP pass 83 on 14 January and EREP pass 89 on 24 January intersected over the southwest corner of Minnesota and parts of Iowa and

South Dakota (see Figure 2-5). This area is representative of the Midwest with relatively flat terrain and most of the land in agricultural production.

Mosaics for this area, made from the S190A visible band negatives are shown in Figures 4-9 and 4-10, respectively. On the earlier date, the entire area is covered by a uniform blanket of snow with depths ranging from 15 to 30 cm (6-12 inches); on the later date snowmelt has occurred in two distinct zones. A band of nearly complete snowmelt (80-90% reduction of snowcover) can be seen in the center of Figure 4-10, whereas only a 50% reduction in snowcover has occurred in the areas to the northeast and southwest of this zone. Although analysis of surface weather charts and climatological data books offered no apparent meteorological explanation for this particular snowmelt pattern, maps of this area suggest a topographic relationship. The areas of heavy snowmelt correlate with contour lines on the map, so the pattern may be partially due to a change in elevation. This area also appears to be dissected by numerous streams and lakes which could create a slightly different soil profile and moisture content resulting in increased snowmelt and runoff.

Visual interpretation of the S190A and S190B photography for the Midwest test site does not suggest that the character or reflectance response of snowcover in this area is significantly different from snowcover in mountainous terrain. It is possible, however, that the lack of topographic relief would minimize the occurrence of areas of deep snow associated with sheltered north facing slopes in mountainous terrain. Also, different soil types and possibly more extensive surface water drainage patterns in the flatter terrain could significantly affect the extent and duration of snowcover in this area.

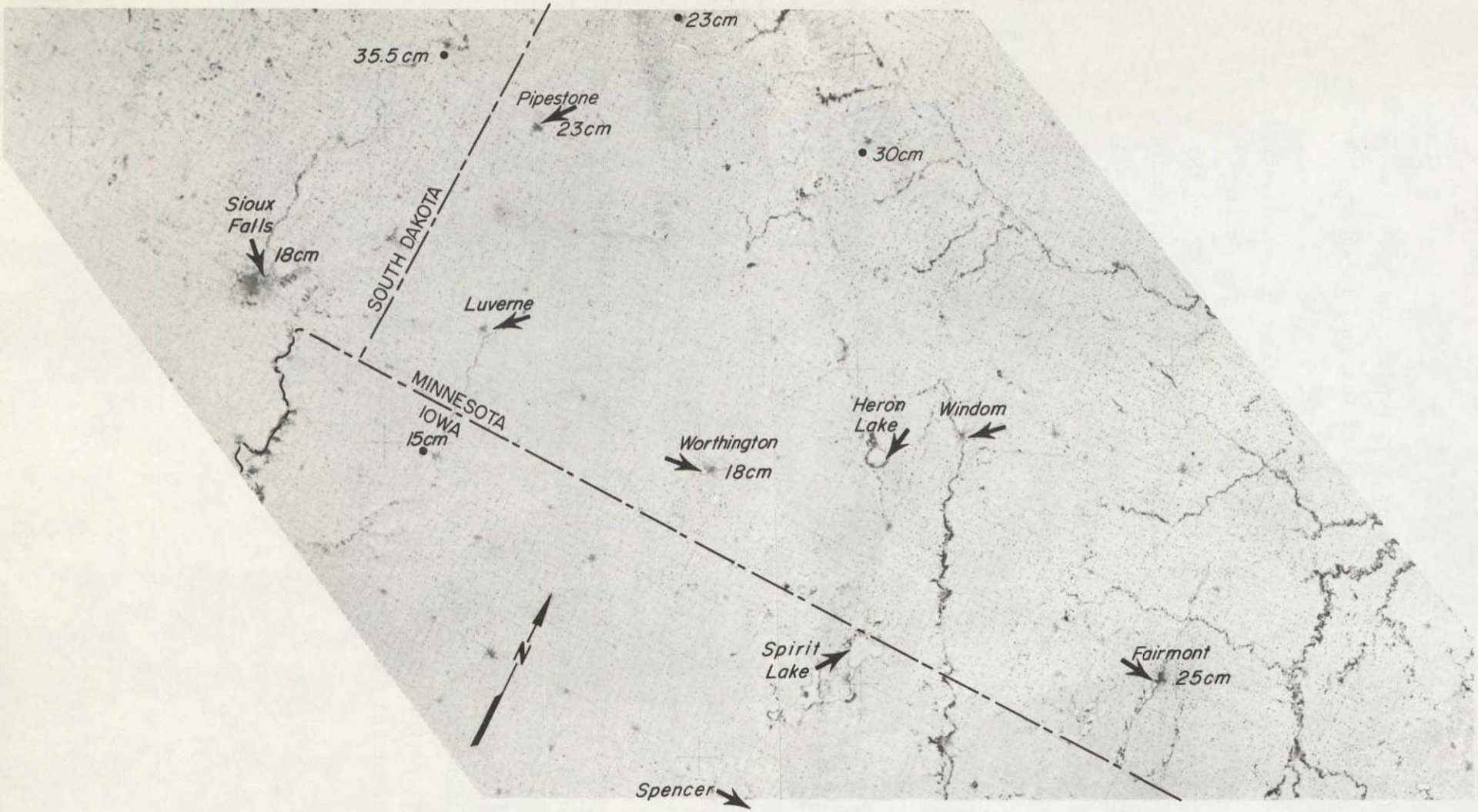

Figure 4-9 S190A Camera Station 6 (0.5 - 0.6 μm) photograph taken on 14 January 1974 (EREP Pass 83) covering a portion of southwestern Minnesota (Test Site 318592). Picture area represents the overlap of EREP passes 83 and 89 (See Figure 2-5). Snow depths are indicated.

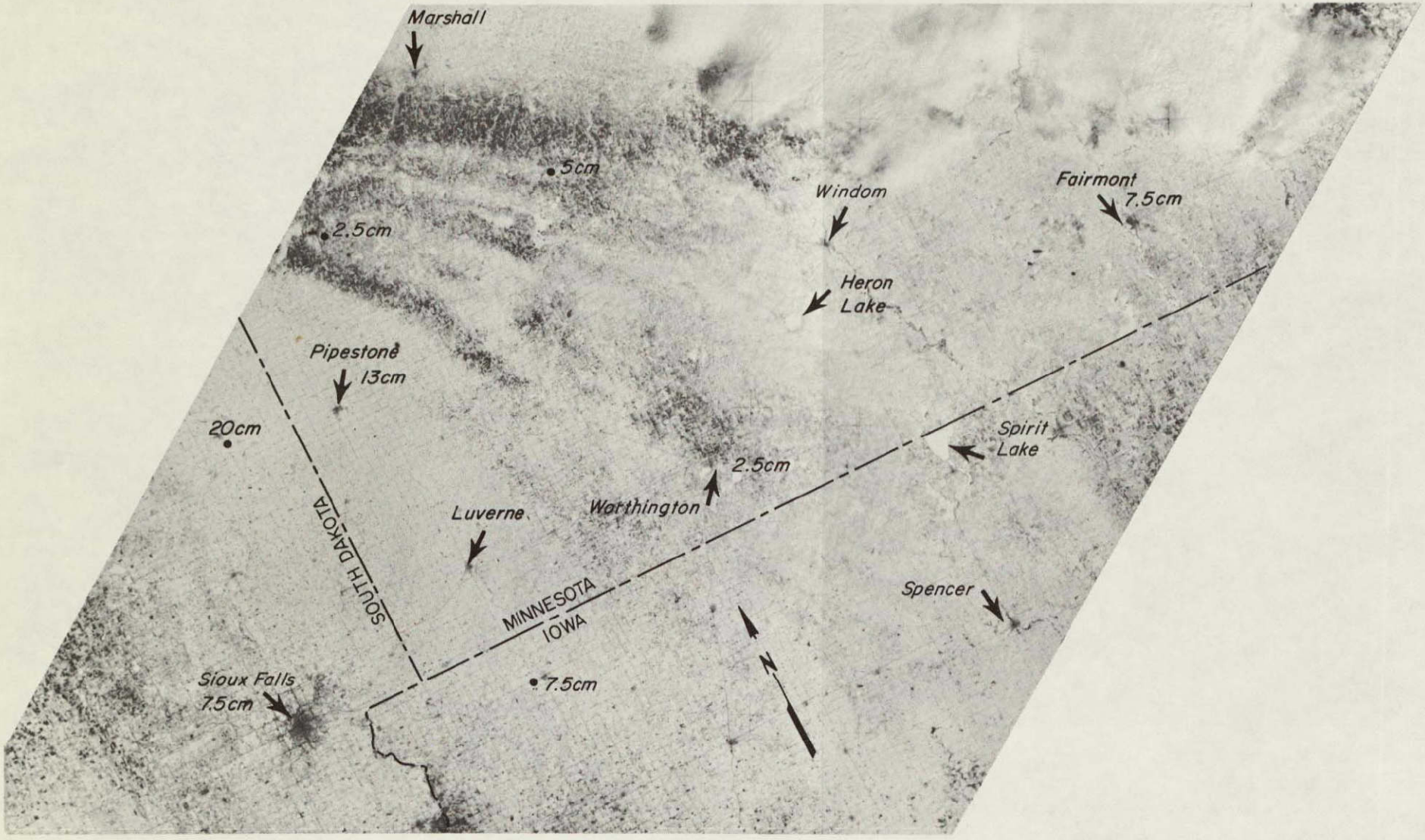

Figure 4-10 S190A Camera Station 6 (0.5 - 0.6 μm) photograph showing same area as previous figure, taken 10 days later on 24 January 1974 (EREP Pass 89). Extensive melting has occurred (northeast of Pipestone) as indicated by reduced reflectance as compared to Figure 4-9.

PAGE INTENTIONALLY BLANK

5. ANALYSIS OF S192 MULTISPECTRAL SCANNER DATA

5.1 Spectral Reflectance of Snowcover

The initial spacecraft measurements in the near-infrared portion of the spectrum were those of the 0.7 - 1.3 μm band of the Nimbus-3 HRIR (High Resolution Infrared Radiometer). In studies reported by Barnes and Bowley (1970), it was first noticed that snowcover could not be distinguished in the HRIR imagery. In a subsequent, more thorough investigation of the HRIR near-infrared data, Strong, McClain, and McGinnis (1970) attributed the observed low reflectance of snow and ice to the existence of melt water; they pointed out that with even a thin layer of water on the snow or ice, the surface would appear highly reflective in the visible portion of the spectrum but essentially non-reflective in the near-infrared.

In an investigation of Landsat-1 imagery (Barnes, Bowley, and Simmes, 1974), the contrast between snow and bare ground was found to be considerably lower in the MSS-7 near-infrared band (0.8 - 1.1 μm) than in the MSS-5 visible band. Despite the lower contrast, however, the snow line in the wintertime images could be mapped from the MSS-7, and the snow extent appeared to be about the same as determined from the MSS-5 data.

In some late spring cases, however, the areas appearing very bright in MSS-7 are significantly smaller than those appearing bright in MSS-5. For example, in the Kern Basin (in the Sierra Nevada) on 30 June 1973, the brightest tones in MSS-7 are limited to the highest ridges, whereas in MSS-5 a distinctly larger area appears to be snowcovered. It was concluded that the snow visible in the near-infrared image may be the high-elevation dry snow, whereas both the dry and lower elevation wet snow surfaces are detectable in the visible image. In a study of several river basins in the Wind River Range in Wyoming (Rango, Salomonson, and Foster, 1975), the Landsat MSS-7 imagery consistently indicated less snowcover than did the MSS-5; the difference was attributed to the reduced near-infrared reflectance associated with melting or refrozen previously melting snow.

Recent laboratory experiments reported by O'Brien and Munis (1973)

TABLE 5-1

S192 MULTISPECTRAL SCANNER
SPECTRAL BANDS

Band Number	Description	Spectral Range (μm)
1	Violet	0.41-0.46
2	Violet-Blue	0.46-0.51
3	Blue-Green	0.52-0.56
4	Green-Yellow	0.56-0.61
5	Orange-Red	0.62-0.67
6	Red	0.68-0.76
7	Infrared	0.78-0.88
8	Infrared	0.98-1.08
9	Infrared	1.09-1.19
10	Infrared	1.20-1.30
11	Infrared	1.55-1.75
12	Infrared	2.10-2.35
13	Thermal Infrared	10.2-12.5

have been conducted to determine the effects of various natural conditions, especially melting and refreezing, on the spectral reflectance of a snowcover in the red and near-infrared regions. The results of these experiments indicate that toward the red end of the visible spectrum, the reflectance declines somewhat and falls off rapidly in the near-infrared region. As fresh snow ages without melting, there is a small decrease in reflectance; if melting occurs to the point of producing a wet snow surface, however, a significant reduction in reflectance is observed.

5.2 S192 Data Sample

5.2.1 Data Formats

The S192 Multispectral Scanner is a 13-band sensor with 12 of the bands being in the visible or near-infrared portion of the spectrum extending to about 2 μm. The thirteenth band is in the thermal infrared. The spectral range for each band is shown in Table 5-1. The conical scan pattern of the S192 covers a swath of the earth's surface that is approximately 72.4 km wide; the instantaneous field of view (IFOV) is 79.25 meters (260 feet).

The S192 data provide for the first time an opportunity to examine the spectral characteristics of snow from space over the spectral range extending from the visible to well into the the near-infrared. For the analysis of S192 data, the film products and Computer Compatible Tapes (CCT's) were both used. Initial analysis was carried out using the 70 mm screening film, which was obtained for only a few of the spectral bands. Later analyses were carried out using the larger scale interim film and the line-straightened final film product. The identification number of the CCT's used in the study are listed in Table 5-2. A complete description of all of these S192 data output products is given in the NASA publication "Earth Resources Production Processing Requirements for EREP Electronic Sensors" (Aerospace and Defense Systems Operations, 1973).

5.2.2 Snowcover Conditions

The EREP passes for which S192 data were collected for use in this

TABLE 5-2

S192 MULSTIPECTRAL SCANNER
DATA SAMPLE

Case Number	Test Site	EREP Pass	Date	CCT Number	Start-Stop Time (G.M.T.)	Approximate Time of Observation (Local Time)
1	318107	3	3 Jun 73	No CCT data available	19:23:54-19:23:59	1130
2	547220	5	5 Jun 73	929772	17:58:09-17:58:13	1100
3	318208	83	14 Jan 74	932700 932701 932702 932703	16:58:59-16:59:18	1000
4	318592	89	24 Jan 74	927258 927259 927260 927261 927262	17:58:19-17:58:51	1200
5	318107	98	1 Feb 74	933026 933027 933028	16:59:03-16:59:24	0900

study include two from the SL-2 mission in June 1973 and three from the SL-4 mission in January-February 1974. It was possible, therefore, to investigate the reflectance characteristics of snow in late spring situations, representative of presumably melting snow, and in mid-winter situations, representative of presumably dryer, colder snow. Digitized data were available for only one of the two SL-2 passes, however; CCT's were not processed for EREP Pass 3 because the sensor was not aligned correctly (film products were available). A complete description of each of the test site areas is given in Section 2.

Since this experiment was designed to examine EREP data collected over relatively large areas, it was not feasible to collect detailed information on the snow conditions at a particular test site. The overall snow conditions can be estimated, however, through routinely collected snow reports (see Section 3.2) and the meteorological conditions prior to and at the time of the Skylab pass. In each case, the limits of the snow cover can be delineated using the S190A and S190B photography, as discussed in Section 4.

For Case 1, the maximum temperature on 3 June at a station located at the 4150 meter level in the White Mountains was 5°C; this station reported a snow depth of 12.5 cm. At a lower station at the 3700 meter level, which reported no snow, the maximum temperature was 12°C. Both of these stations had minimum temperatures below freezing during the previous night. It is probably that the snowpack consisted of refrozen snow with perhaps some melting taking place, especially at the lower levels, at the time of the EREP pass (1130 LST).

The snow conditions for Case 2, in the Wasatch Range, appear to be similar to those in the White Mountains. The maximum temperature at a reporting station at the 1700 meter level on 5 June was 24°C. Assuming a lapse rate of 10°C per km, the temperature at even the highest peaks (3700 meters) would be somewhat above freezing. The snowpack would almost certainly have been in a melting condition at 1100 LST, the time of the EREP pass, except perhaps at the highest elevations not facing the sun.

In central Arizona test site area (Case 3), cold weather with continuous below freezing temperatures had prevailed during the first 10 days of January. A warming trend then set in on the 11th, with

temperatures reaching above freezing as high as the 2500 meter level on each day from the 11th through the 14th. The maximum at a station at 2493 meters on the 14th, the day of the EREP pass, was 10.5° C; temperatures during the night were well below freezing, however, being as low as -18° C on the 11th and 12th. Snow had fallen in the area on the 9th and 12th of January, but the reported snow depth at Flagstaff had decreased from 68 cm on the 10th to 43 cm on the 14th. Even in mid-January, therefore, some melting could have taken place in the central Arizona mountains, although snowfall had occurred only five days prior to the Skylab pass.

In the Midwest case, maximum daytime temperatures had been running near the freezing level from the 18th through the 24th, with minimum nighttime values well below freezing. Light snowfalls had occurred during the period of the 14th to the 24th, although the reported snow-cover in the area generally decreased a few centimeters during this period, due to a warm spell on the 16th and 17th. The snow conditions at the time of the Skylab pass on 24 January were probably stable, therefore, with no melting taking place. The S190A photography of this area is discussed in detail in Section 4.4.4.

The final case, on 1 February, is in the area of Walker Lake, near the California-Nevada border. At the end of January, daytime temperatures at a station at the 2167 meter level, were as high as 12° C, but were constantly below freezing at night. In the highest mountains (e.g. the stations in the White Mountains), temperatures had been continuously below freezing. The last substantial snowfall had occurred about 10 days before the Skylab data were collected.

In summary, meteorological data indicate the snow cover in the test site areas observed in June 1973 was quite probably in a melting condition, except perhaps at the highest elevations. In each of the test site areas observed in mid-winter, some melting could have been taking place at lower and middle elevations, or the snowpack could have been refrozen from melting that has occurred during the preceeding few days. However, the snow conditions were more stable than in the two springtime cases. No S192 data were collected over a test site area immediately following a fresh snowfall or during a very cold period.

5.3 Analysis of S192 Imagery

5.3.1 Analysis Procedures

The initial visual interpretation of the S192 data was carried out using the 70 mm screening film. Although the screening film was not intended to be a high quality product, and only three or four spectral bands were provided for each case, the differences in snow reflectance in the visible and near-infrared were, nevertheless, detectable. The screening film was also used to specify the segments of each pass for which the later film products and CCT's were requested. Visual interpretation of the larger scale interim and final film products was subsequently carried out to examine more closely the band-to-band variations in snow reflectance. The analysis of the S192 imagery concentrated on the interpretation of the near-infrared bands; the data from the thermal infrared band were not analyzed in detail because the earlier measurements were of poorer quality than those of the other bands.

In order to obtain a more objective interpretation of the imagery, densitometric analysis was also carried out using the larger-scale film transparencies. A standard-type densitometer with a 1 mm spot size was used for the analysis.

5.3.2 Results of Visual Interpretation

5.3.2.1 SL-2 EREP Passes

The preliminary S192 screening film received early in the study period displayed a marked drop in the reflectance of snow in the near-infrared bands. This effect is readily apparent in the imagery from the two SL-2 EREP Passes, over the Sierra Nevada-White Mountain area and the Wasatch area, respectively.

The snowcover in the Wasatch area is delineated in the S190A photograph shown in Figure 5-1; the S192 Band 2 and Band 11 imagery is shown in Figures 5-2 (a and b). Similarly, the Sierra Nevada-White Mountains area is shown in the S190A photograph in Figure 5-3; the S192 Band 2 and Band 11 imagery for the White Mountains is shown in Figures 5-4 (a and b). In both cases, snowcover has a high reflectance in the visible band, but appears essentially black in the near-infrared.

Figure 5-1 S190A Camera Station 6 (0.5 - 0.6 μm) photograph from EREP Pass 5, 5 June 1973; area covered includes the Wasatch Plateau and Mt. Nebo Range in Utah.

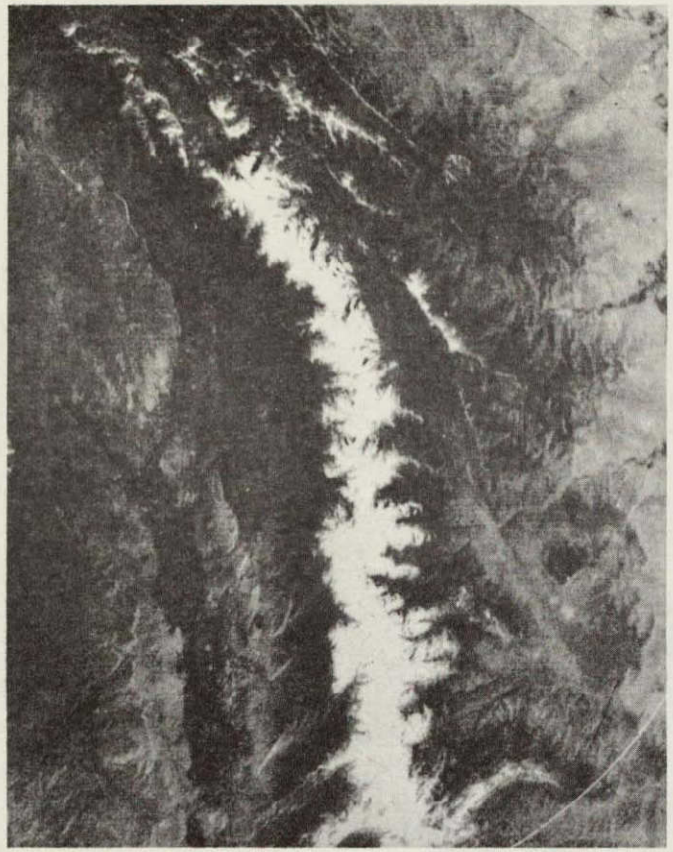

(a) Band 2

(b) Band 11

Figure 5-2 S192 imagery from EREP Pass 5, 5 June 1973; (a) Band 2 (0.46 - 0.51 μm), (b) Band 11 (1.55 - 1.75 μm). Area covered is the Wasatch Range in Utah. Note decreased reflectance of snow in Band 11 as compared to the Band 2 imagery.

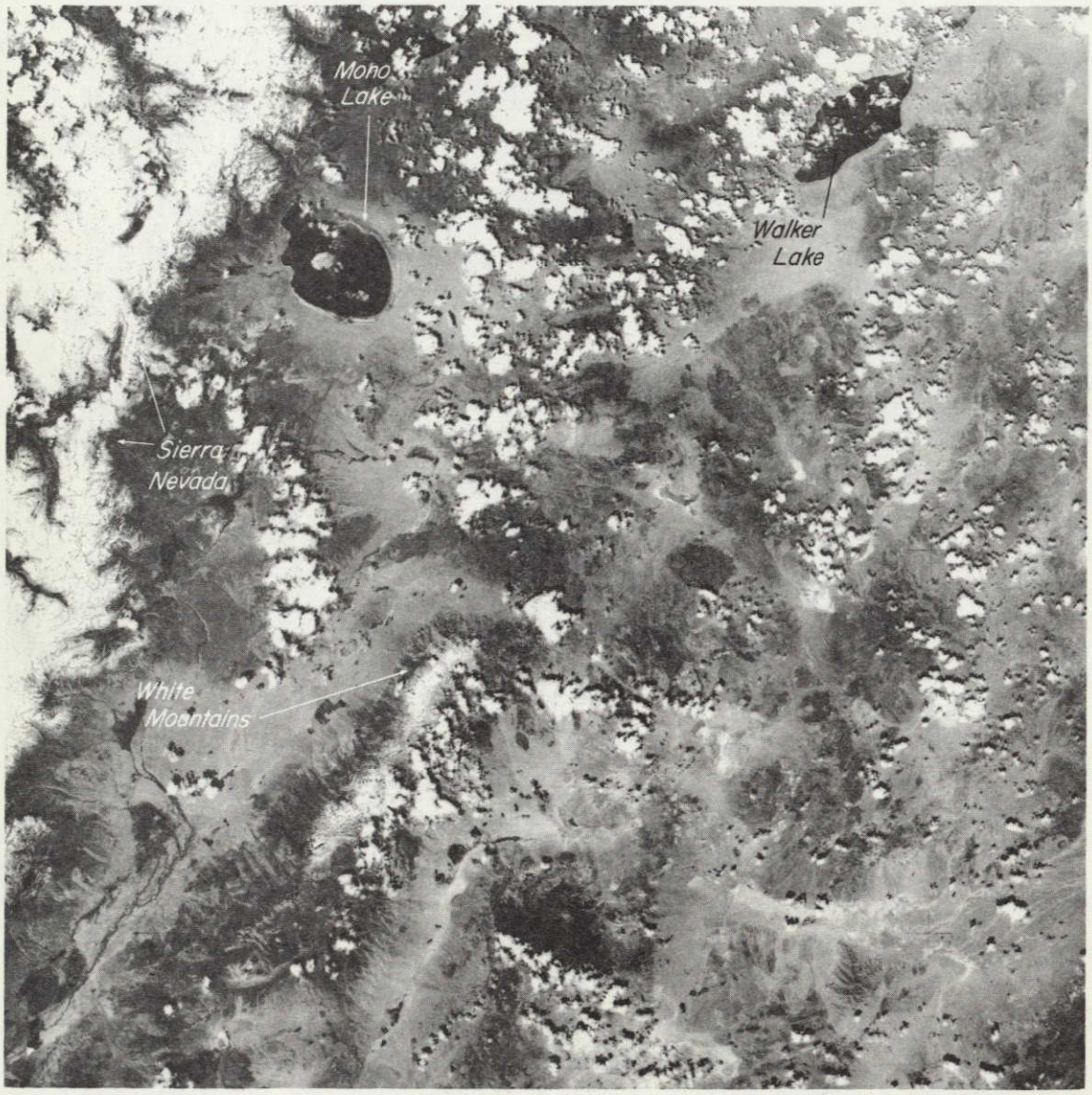

Figure 5-3 S190A Camera Station 6 (0.5 - 0.6 μm) photograph from EREP Pass 3, 3 June 1973; area covered includes the White Mountains and Walker Lake.

(a) Band 3

(b) Band 11

Figure 5-4 S192 imagery from EREP Pass 3, 3 June 1973; (a) Band 3 (0.52 - 0.56 μm), (b) Band 11 (1.55 - 1.75 μm). Area covered is the White Mountains. Because of the decreased reflectance of the snow, clouds that cannot be detected in Band 3 are distinct in Band 11.

In the Pass 3 imagery (Figures 5-3 and 5-4), not only is the difference in the reflectance of the snow between the visible and near-infrared bands dramatic, but also the distinct nature of the clouds in the near-infrared spectral region is apparent. The S190A photograph indicates that cellular type clouds, a pattern representative of cumulus (water clouds) cells, cover much of the area. Over the mountains, it is difficult to distinquish between the clouds and the snow. The same is true in the visible band S192 imagery, where the clouds and snow have essentially the same reflectance. In the Band 11 imagery, however, the clouds still appear white whereas the snow appears essentially black; therefore, each cumulus cell is distinct, even those cells directly over the snow-covered mountains.

In the initial interpretation of the Case 1 screening film, it was also noticed that in Band 9 some snow can be detected, but the extent of the snow appears to be less than in the visible band. The complete spectral coverage of the line-straightened imagery permitted a more thorough investigation of the snow reflectance in the intermediate bands between the visible and Band 11. In Figures 5-5 a (through f), the images for Bands 3, 7, 8, 9, 10, and 11 from Pass 5 are shown. The area covered includes the Mt. Nebo Range and San Pitch Mountains in the Wasatch Range. In the visible, the entire snowpack has a high reflectance and the snow extent if equivalent to that seen in the S190A photography (Figure 5-1). In Band 7, however, a slight decrease in the apparent snow extent in the Mt. Nebo Range is observed; in Bands 8, 9 and 10, the apparent snowcover successively decreases until in Band 10, the only bright area is along the highest ridge of the range; in Band 11, no snow can be detected. In the San Pitch Mountains, which are at a lower elevation, the less extensive snowcover can barely be detected in Band 7 and cannot be detected in Bands 8 through 11.

5.3.2.2 SL-4 EREP Passes

Both the interim film and final film products were received for the EREP Pass over the Arizona test site in mid-January. The interim film covers the area extending from the Gulf of California to the southeastern corner of Colorado; in the latter part of this pass

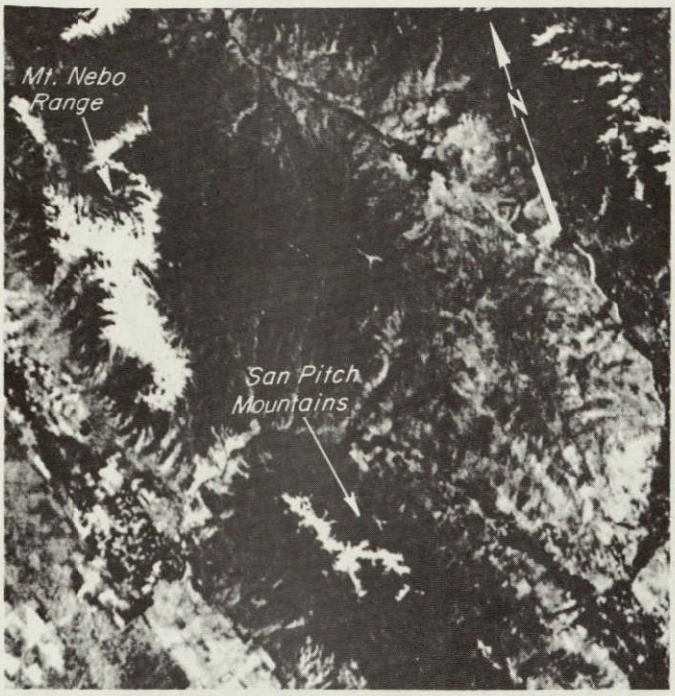

(a) Band 3

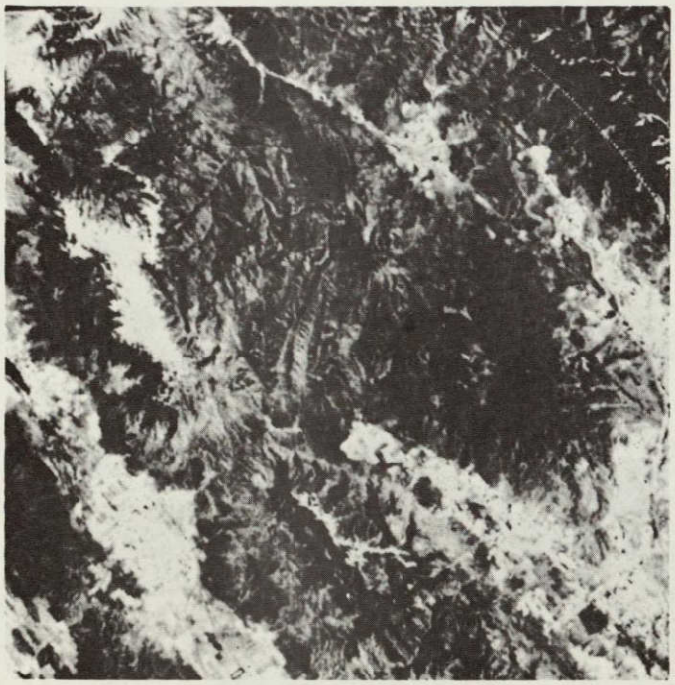

(b) Band 7

Figure 5-5 S192 imagery from EREP Pass 5, 5 June 1973; area covered includes the Mt. Nebo Range and San Pitch Mountains in Utah. (a) Band 3 (0.52 - 0.56 μm), (b) Band 7 (0.78 - 0.88 μm), (c) Band 8 (0.98 - 1.08 μm), (d) Band 9 (1.09 - 1.19 μm), (e) Band 10 (1.20 - 1.30 μm), and (f) Band 11 (1.55 - 1.75 μm). Note the gradual decrease in the extent of snowcover that maintains a high reflectance from Bands 3 through 11.

(c) Band 8

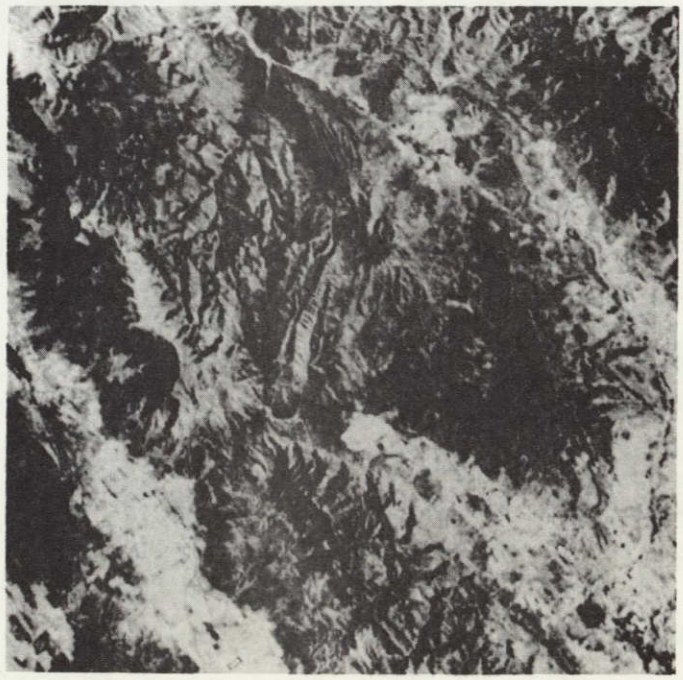

(d) Band 9

Figure 5-5 continued

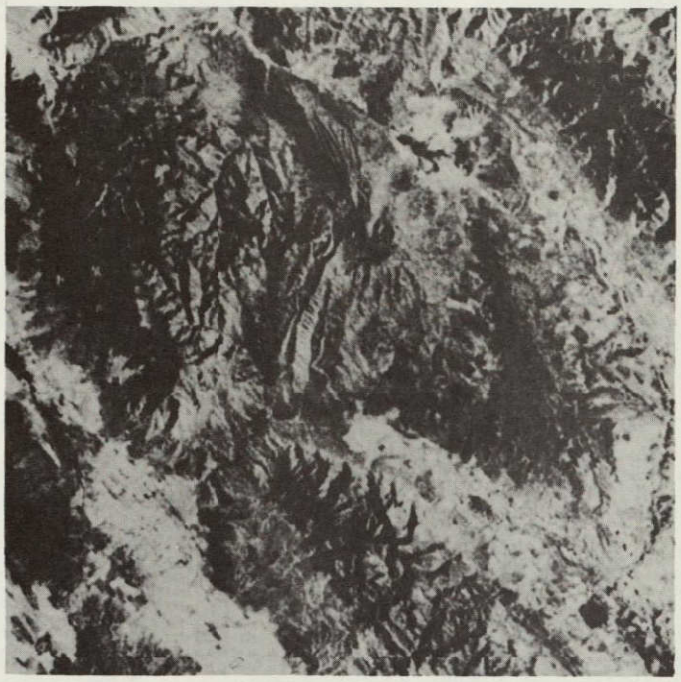

(e) Band 10

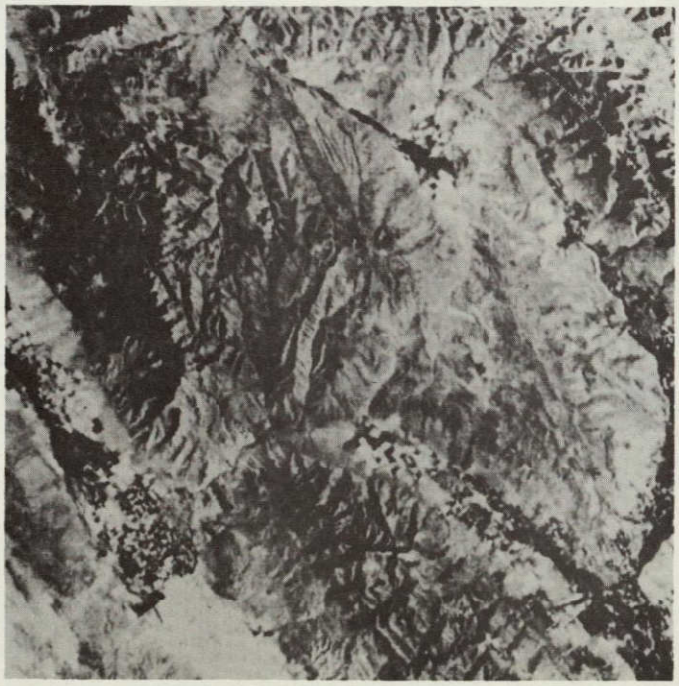

(f) Band 11

Figure 5-5 continued

(a) Band 6

(b) Band 9

Figure 5-6 S192 imagery from EREP Pass 83, 14 January 1974; area covered includes the central Arizona mountains. (a) Band 6 (0.68 - 0.76 μm), (b) Band 9 (1.09 - 1.19 μm), (c) Band 10 (1.20 - 1.30 μm), and (d) Band 12 (2.10 - 2.35 μm). Note the gradual decrease in the reflectance of the snow-cover.

(c) Band 10

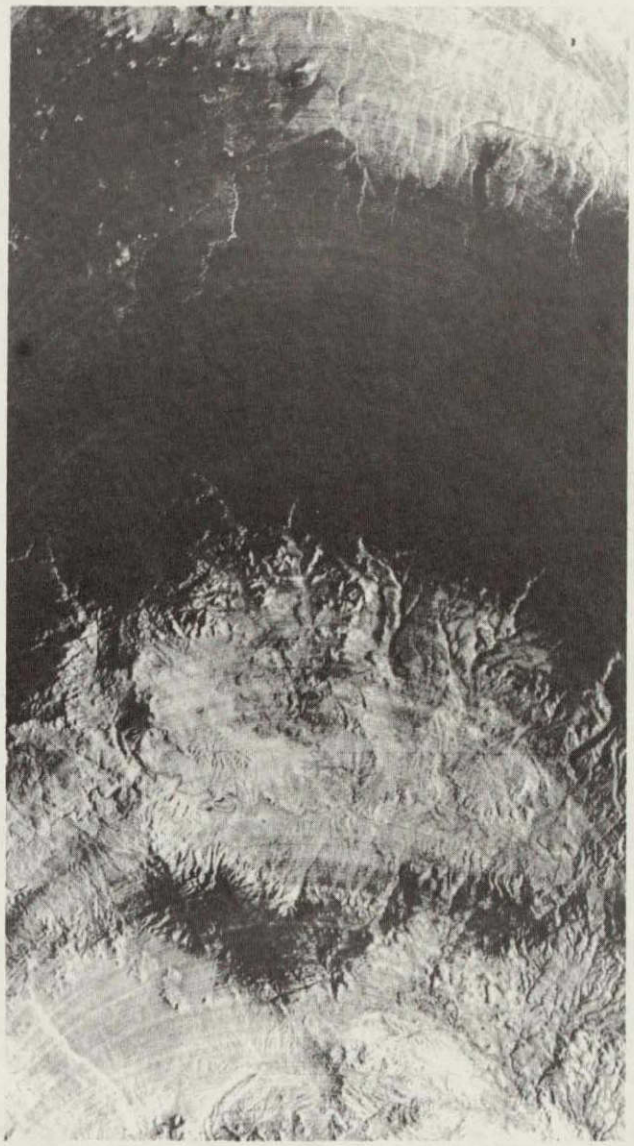

(d) Band 12

Figure 5-6 continued

stratus-type cloud can be seen in the lower valleys with snow on the higher mountains. The final imagery covers the immediate area of the Salt-Verde Watershed, where no clouds existed. The S192 Bands 6, 9, 10, and 12 are shown in Figures 5-6a through 5-6d.

The results of the visual interpretation of the Arizona imagery are similar to those for the SL-2 data discussed above. As seen in Figure 5-6a, snow has a high reflectance except in areas that are forested (the snow patterns and forest effects in the central Arizona area are discussed in more detail in Section 4). In the Band 12 imagery, the entire snowcovered area is non-reflective. In the intermediate spectral bands, a gradual lowering of the reflectance is observed beginning with about Band 8 or 9; however, the decrease in reflectance is uniform across the snowcover, and no gradual decrease in the apparent snow extent is observed, as was the case in the data from each of the SL-2 passes. In the southern Colorado area, the reflectance of the stratus cloud is considerably higher than the snow reflectance in the near-infrared bands.

Similar results were observed for the two other SL-4 cases. EREP Pass 98 crossed an area between Mono and Walker Lakes in which clouds and some snowcover existed. Based on interpretation of the S190A photograph (Figure 5-7), the snowcover in this area does not appear to be substantial and is limited to the higher ridges. Again, the snow exhibits a sharp decrease in reflectance in Bands 10, 11, and 12, whereas the cloud bands remain highly reflective; the imagery for Bands 6 and 11 is shown in Figure 5-8 (a and b). In Case 4, EREP Pass 89 crossed essentially continuous snowcover in the Mid-west; in this case, the reflectance of the entire S192 film segment dropped off in the near-infrared bands.

5.3.3 Results of Densitometric Analysis

The results of the densitometric analysis of the final film products present a more objective interpretation of the snow reflectance characteristics. A graph of the film density values measured in the central Arizona area (Case 3) is shown in Figure 5-9. The graph indicates that snow in non-forested areas (A) tends to maintain a high reflectance in the visible bands until it begins to drop off in Bands 9

Figure 5-7 S190A Camera Station 6 (0.5 - 0.6 μm) photograph from EREP Pass 98, 1 February 1974; area covered includes Walker Lake. Note the reflectance similarities between snow and clouds.

761547

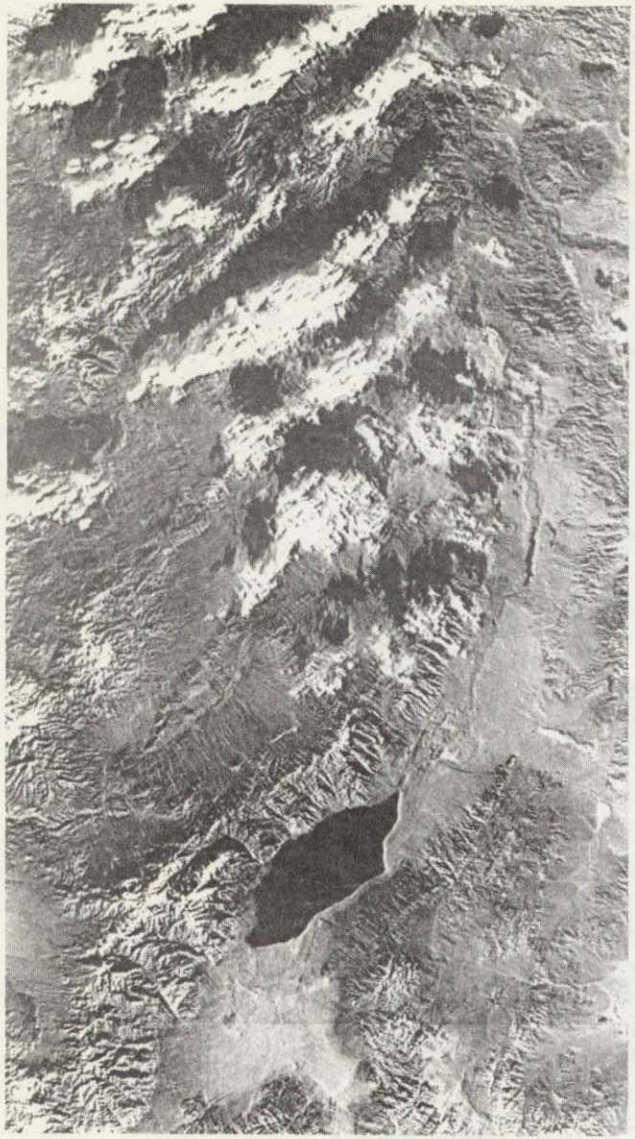

(a) Band 6

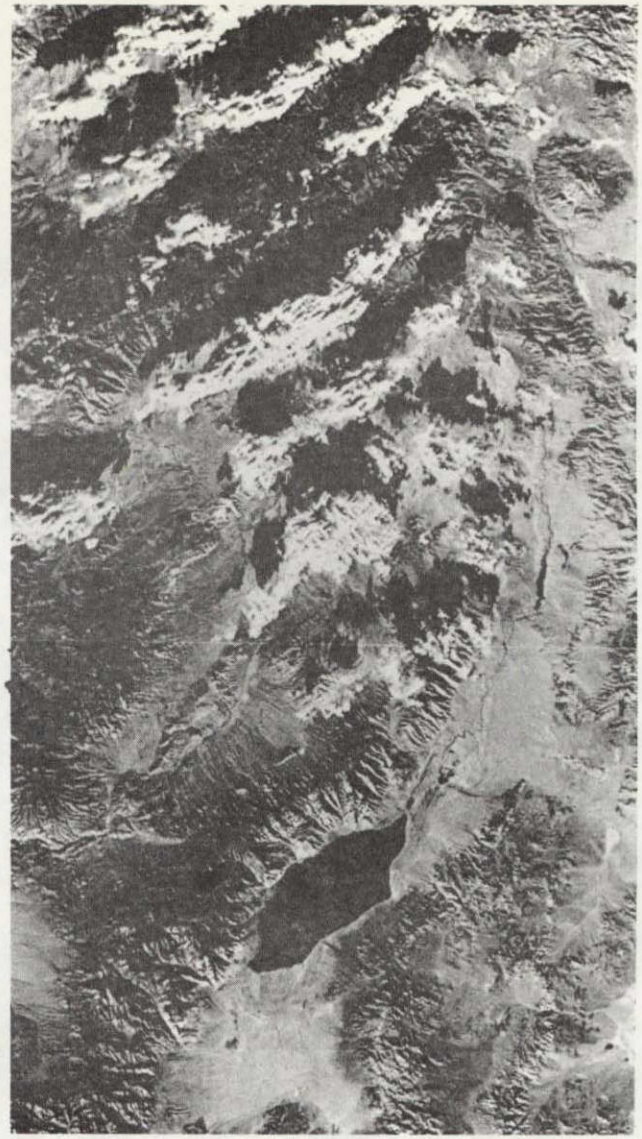

(b) Band 11

Figure 5-8 S192 imagery from EREP Pass 98, 1 February 1974; area covered includes Walker Lake and a portion of the Sierra Nevada. (a) Band 6 (0.68 - 0.76 μm), and (b) Band 11 (1.55 - 1.75 μm). Both snow and clouds have a high reflectance in Band 6; whereas only clouds maintain a high reflectance in Band 11.

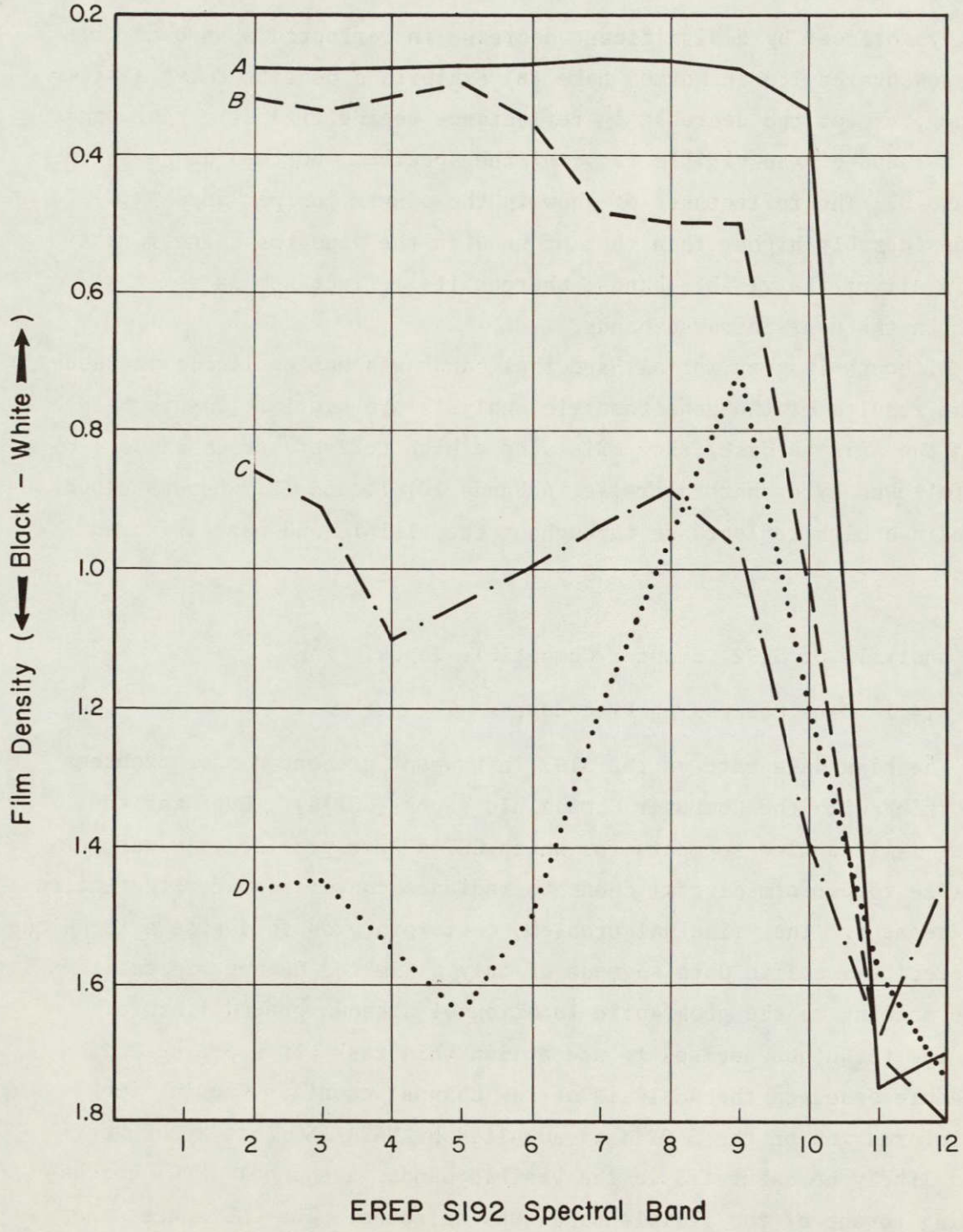

Figure 5-9 Graph showing film density vs. S192 spectral band for (A) uniform snowcover, (B) snowcovered ice on Mormon Lake, (C) snow in Pinyon Juniper forest, and (D) snow in Ponderosa Pine forest (EREP Pass 83, central Arizona test site).

751458

and 10, followed by a significant decrease in reflectance in Band 11. The snowcovered ice in Mormon Lake (B) exhibits a density curve similar to snow, except the decrease in reflectance begins gradually near Band 6 at the end of the visible range of the spectrum and then drops sharply in Band 9. The reflectance of snow in the pinyon juniper forest (C) is considerably higher than that of snow in the ponderosa pine forest (D) in all of the visible bands, whereas its reflectance is somewhat lower in the near-infrared bands.

Although imagery for all spectral bands was not available in Case 5, the results of the densitometric analysis are similar (Figure 5-10). As in the Arizona case, snow maintains a high reflectance in Bands 4 to 9, followed by a sharp decrease in Bands 10, 11 and 12, whereas clouds maintain a high reflectance throughout the visible and near-infrared bands.

5.4 Analysis of S192 Computer Compatible Tapes

5.4.1 Data Processing Procedures

The high data rate of the S192 instrument presented some problems in working with the Computer Compatible Tapes (CCT's). Even for the rather limited time segments for which CCT's were provided, it was not feasible to perform digital count to radiance conversions for the entire data segment. The principal problem, therefore, was to devise a technique to select a specific data segment of only a limited number of scanlines corresponding to the geographic location of a known ground feature.

The technique devised to accomplish this task was a pre-selection procedure based on the analysis of raw channel counts. Knowing from the information on the S192 data supplied by NASA/JSC that snowcover would likely be saturated in the visible bands, a channel (SDO) corresponding to one of the visible bands was selected. The CCT's were then manipulated such that each pixel in that channel that was saturated (raw data count = 255) would be printed out as a black dot and each pixel that was not saturated (raw data count < 255) would be left blank. The result produced an image-like printout where all snowcovered (non-forested) areas appear black.

An example of one of the printouts for the central Arizona area

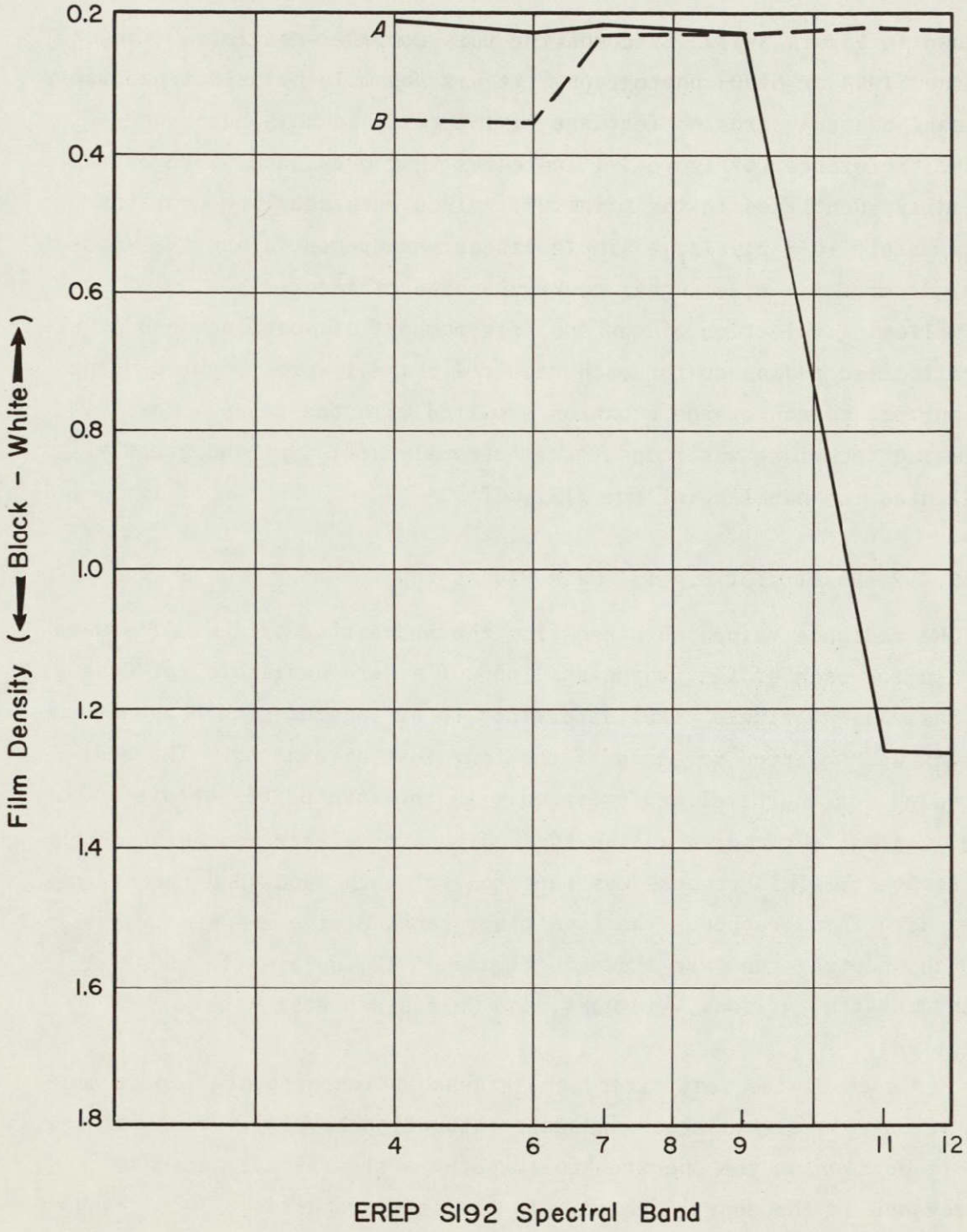

Figure 5-10 Graph showing film density vs. S192 spectral band for (A) snowcovered terrain and (B) clouds in the Walker Lake area (EREP Pass 98).

751459

is shown in Figure 5-11. By comparing this computer-generated "image" with the S190A or S190B photography, it was possible to select precisely the scanlines that crossed features of interest, in this case snowfields. Reference to Figure 4-1 indicates that many snow patterns can be readily identified in the printout. Since each scanline contains approximately 1038 pixels, a simple linear measurement along the scanline indicates the pixels that cover the area of interest.

Following selection of the specific numbers of scanlines and pixels, the calibrated radiances for each required channel were computed using the appropriate conversion equation supplied with the tapes. This processing technique was found to be extremely efficient and greatly facilitated the handling of the S192 CCT's.

5.4.2 Results of Digital Data Processing

The radiance values obtained from the processing of the CCT's were analyzed for each of the four cases (no CCT's were available for Case 1, EREP Pass 3). A single pixel determined to be located within a uniform snowpack was selected for each of the four test site areas. The radiance value for the pixel was averaged with the five pixels before and after it along the same scanline to acquire a true representation of the snow response. This process was repeated for each band, and the averaged values were then graphed. The resulting graphs of the radiance values for each spectral band are shown in Figures 5-12, 5-13, 5-14, and 5-15 for the Wasatch, Arizona, Mid-west, and California test site areas, respectively.

For each of the test sites, the graphs indicate saturation or near saturation values (triangles indicate saturation levels) throughout the visible portion of the spectrum followed by a significant decrease in reflectance in the near-infrared. In the interpretation of the graphs it is necessary to consider not only the curve itself, but also the curve in relation to saturation levels; in this way, a saturated value is not misinterpreted as a decrease in reflectance (such as Band 4).

In the results for Case 2 (Figure 5-12), the first radiance values that are not at the saturation level are in Bands 6 and 7, and the first significant drop in reflectance is in Band 8. In Case 3 (Figure 5-13), the radiance exhibits a substantial drop in Band 8. In both of these

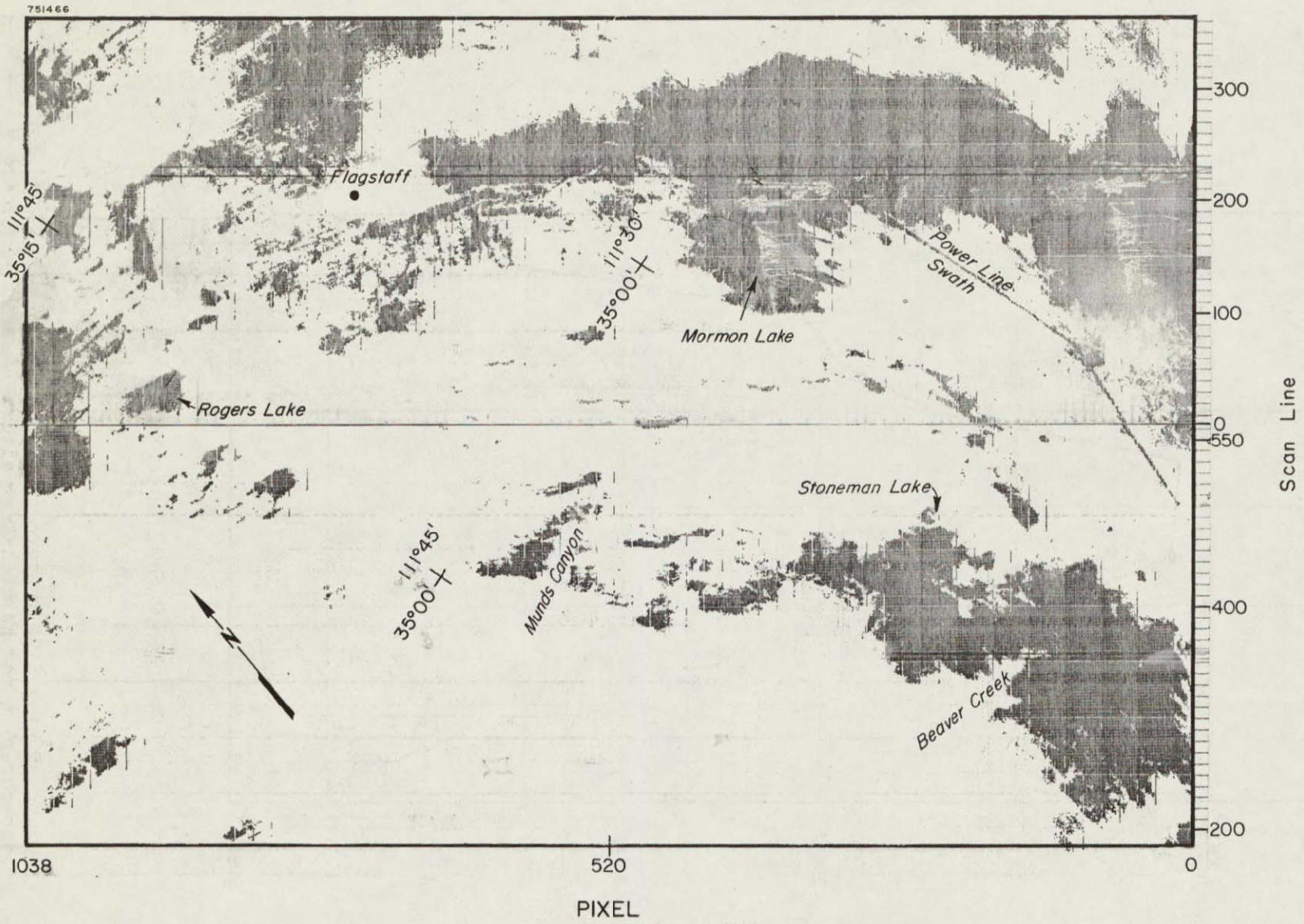

Figure 5-11 Computer printout image derived from S192 visible band raw data. Saturated values (data count = 255) appear black. Snow covered terrain and other highly reflective features can be identified when image is compared with S190A photograph of same area (Figure 4-1).

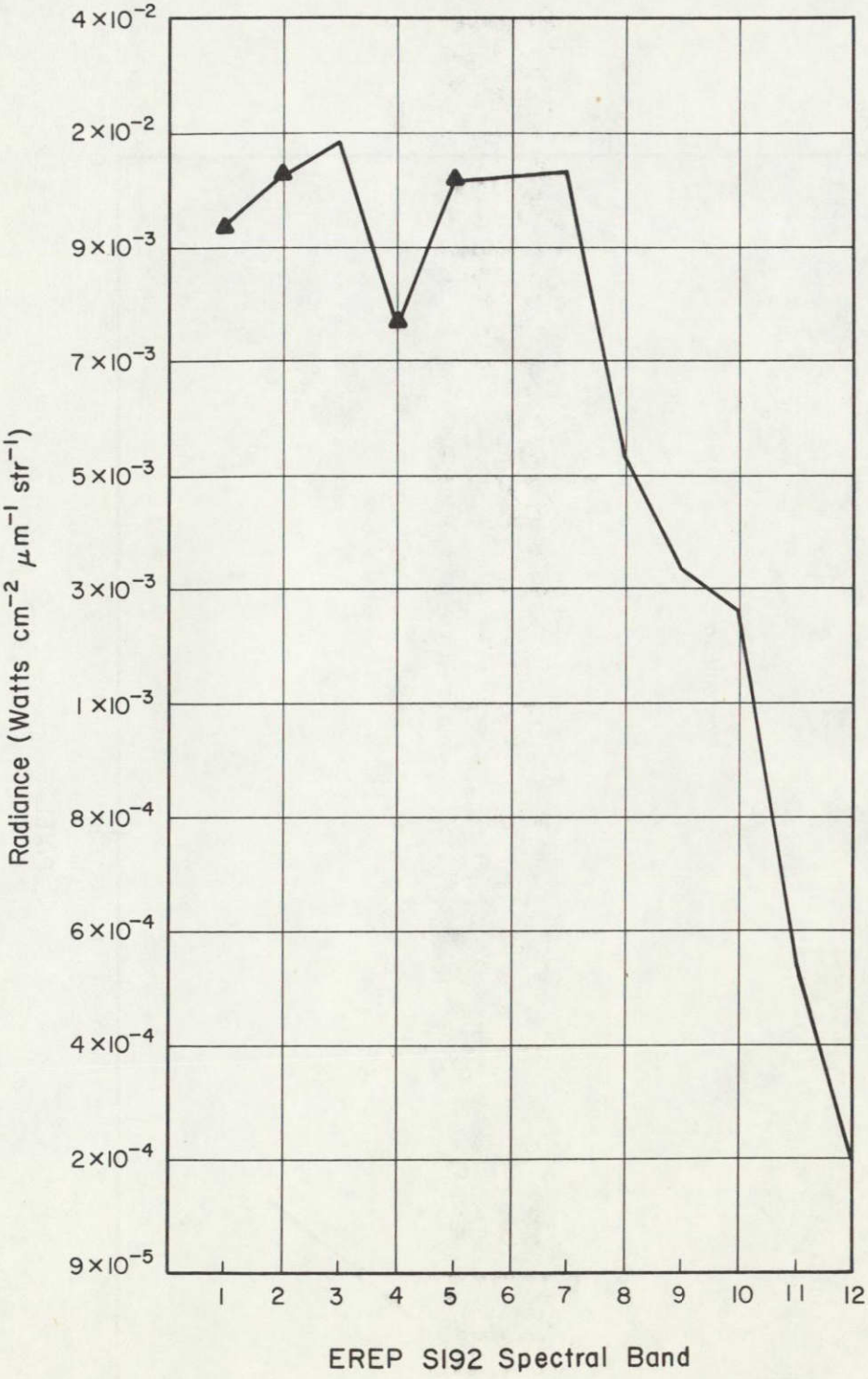

Figure 5-12 Graph showing S192 measured radiance vs. spectral band for snowcover in the Wasatch test site. Triangles indicate saturated values.

751465

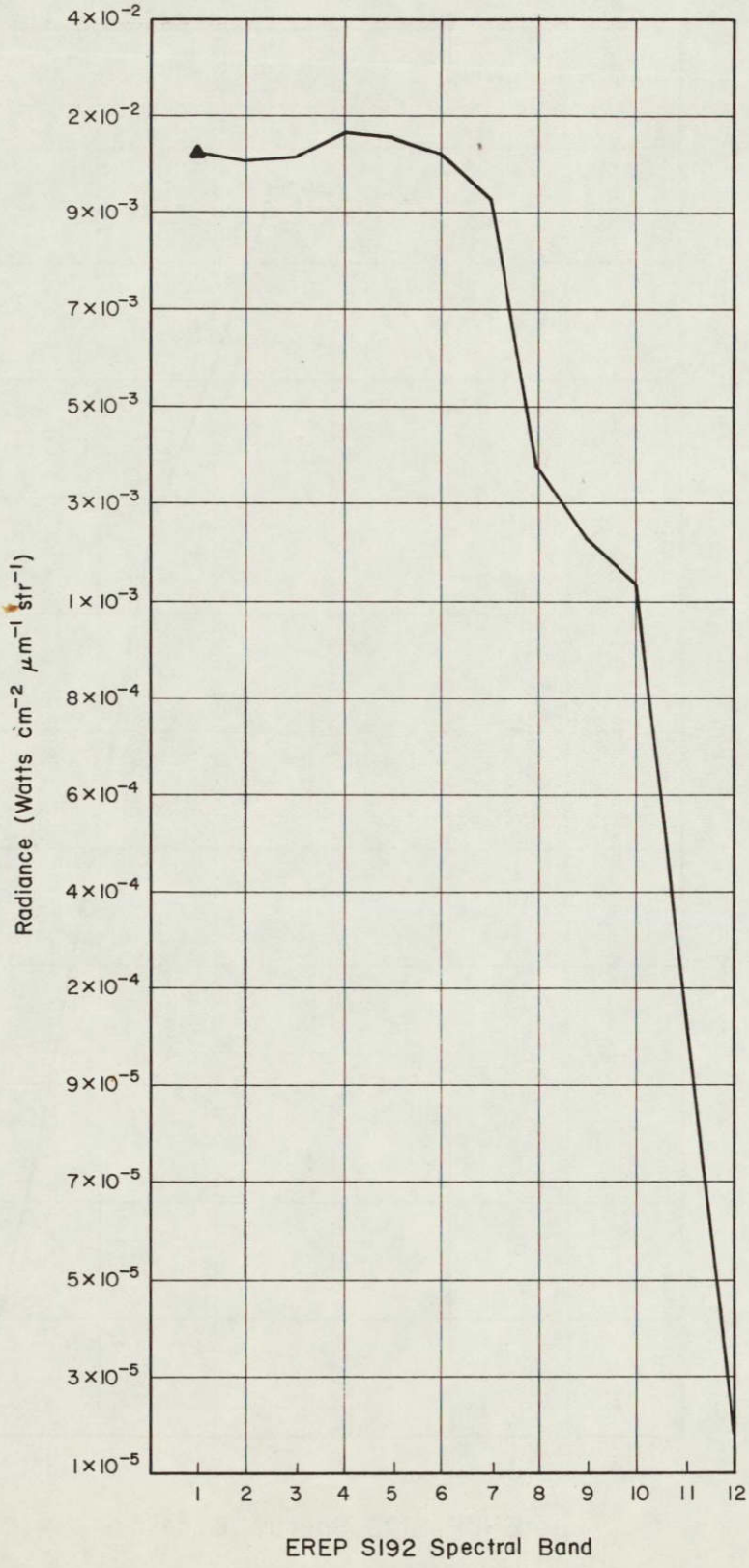

Figure 5-13 Graph showing S192 measured radiance vs. spectral band for snowcover in the central Arizona test site. Triangles indicate saturated values.

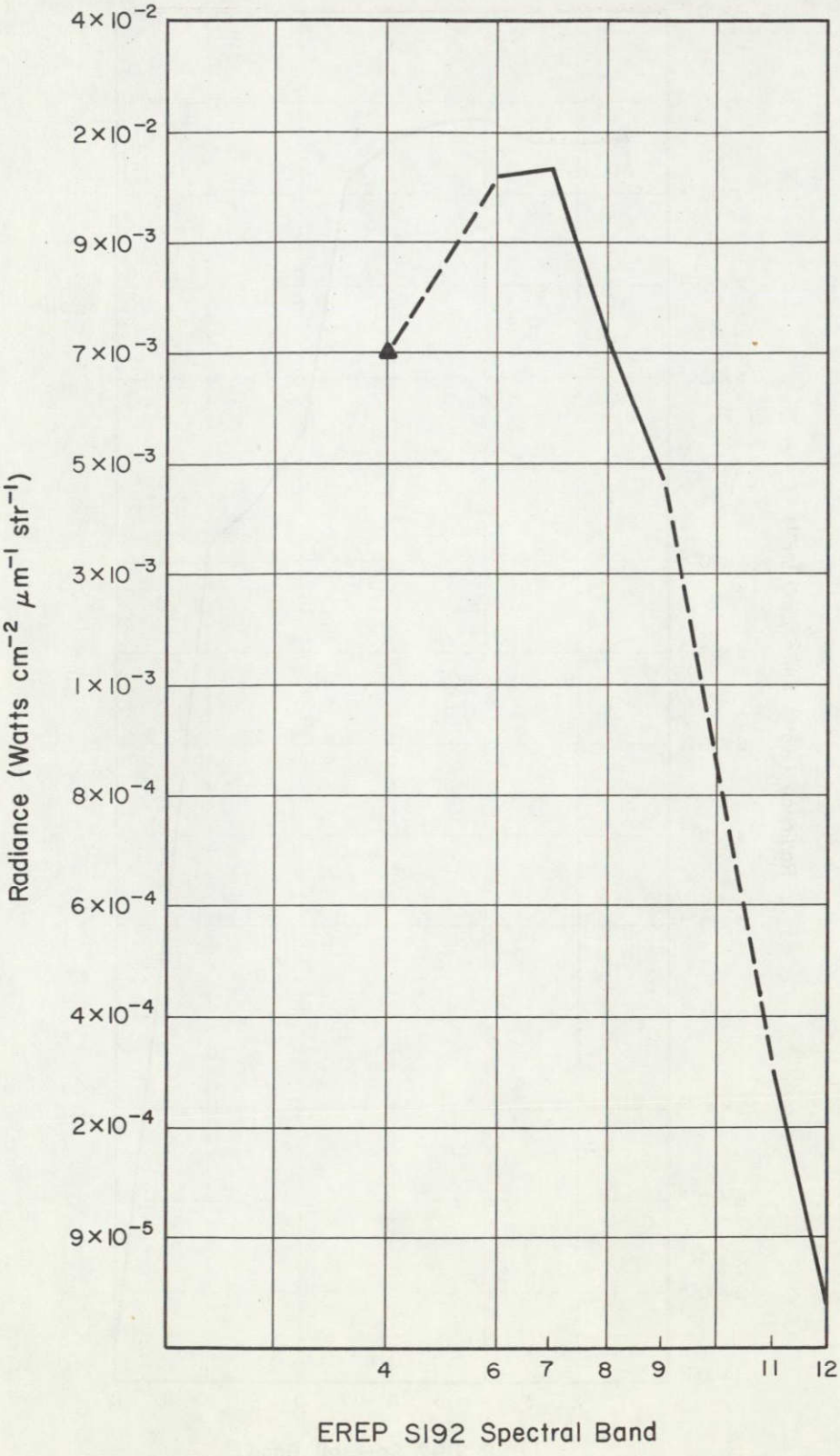

Figure 5-14 Graph showing S192 measured radiance vs. spectral band for snowcover in the Midwest test site (dashed lines indicate spectral bands for which no data were available). Triangles indicate saturated values.

751464

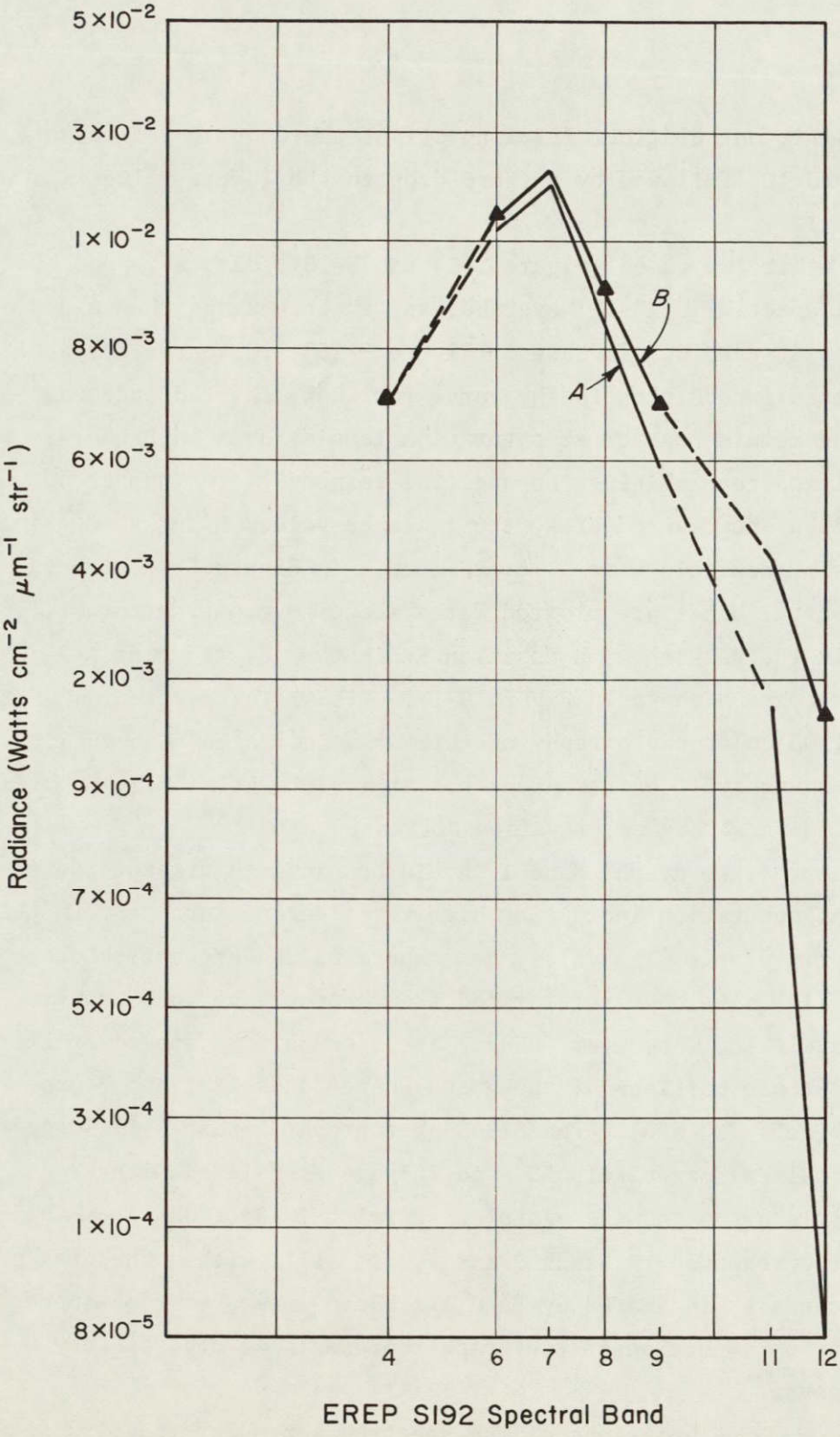

Figure 5-15 Graph showing S192 measured radiance vs. spectral band for (A) snowcover and (B) clouds in Sierra Nevada-Walker Lake test site (dashed lines indicate spectral bands for which no data were available). Triangles indicate saturated values.

cases, a slight, but distinct leveling off of the drop in reflectance occurs at Band 10, followed by a sharp drop to the lowest values in Bands 11 and 12.

In the other two cases (Figure 5-14 and 5-15), data were not available for all spectral bands. Nevertheless, in both cases the values begin to drop at Band 8. In Case 5 (Figure 5-15), the curve for a cloud area is plotted in addition to the curve for snow; the radiance values for the cloud remain near or at saturation levels, even in Band 12.

In addition to examining the spectral response for a number of pixels within a snowcovered area, the radiance values along a scanline that crosses a snowfield were also examined. In Figure 5-16, the values for five spectral bands are plotted for a scanline crossing the Mt. Nebo range in the Wasatch at a position indicated by the line A-A' in the S190A photograph shown in Figure 5-17. Visual interpretation of S190A and S190B color photography of this area indicates that a fairly uniform snowcover still exists along the higher elevation ridges, with the snow becoming patchy as elevation decreases.

To interpret the graph, Band 1 should be examined first to determine areas of saturation indicating highly reflective surfaces, in this case snowcover (pixels 715-845). Areas where values are not saturated (pixels 700-714) have been interpreted from photography to be non-forested slopes with no snowcover. Next, areas of uniform snowcover are indicated by those portions of the graph where Bands 1, 2 and 7 appear saturated (pixels 720-820). The S190A photograph (Figure 5-1) suggests that the anomalies near pixels 757 and 767 are associated with areas in which little or no snow is visible. Pixels 820-840, which exhibit a very erratic response in Bands 2 and 7, are still within the area of high reflectance as indicated by Band 1. Photo-interpretation supports the idea that this portion of the graph represents an area of very patchy snowcover.

The near-infrared portions of the spectrum sensed by the S192 scanner are represented by Bands 10 and 11 on the graph. Starting at pixel 700, a stable response in both Bands occurs along the non-forested slope, followed by a decrease in reflectance as the solid snowpack is reached. Since the two anomalies discussed above (at pixels 757 and 767) exhibit a high reflectance in Band 11 there is further indica-

tion that these areas have no snowcover. Within the areas indicated in photograph to be the pixels where the visible bands have a low reflectance, Band 11 has a corresponding high reflectance; this tendency is similar to the response for the non-forested, non-snowcovered area represented by pixels 700-715. On the other hand, high reflectance in the visible bands corresponds to a low reflectance in Band 11, a characteristic response for areas of snowcover.

The radiance values along segments of scanlines for each test site area are compared in Figures 5-18 (a through d). These segments were determined from interpretation of the S190A photography to be within snowcovered areas. The exception may be Case 5, near the Walker Lake area, where the snow extent is limited, so that the scanline segment may not lie completely within a uniform snowcover. This could account for the erratic values for certain of the bands in that case.

Overall, the radiances are similar for each test site area, with the visible bands being at or near saturation and Band 11 and 12 having the lowest values. The values for Case 3 are consistently lower than those for the other cases; for example, Band 4 is saturated in each case except Case 3, and the values for Bands 7, 9, and 10 are consistently lower than those for the other cases.

5.5 Discussion of Results of S192 Data Analysis

5.5.1 Reflectance Characteristics of Snow

For the five cases for which S192 data were analyzed, the overall results of the analysis of the imagery and the digital radiance values are consistent. In each case, snowcover exhibits a marked drop in reflectance in the near-infrared portion of the spectrum. The digital analysis shows that snow reflectance is high through Band 7, begins to drop in Band 8, levels off somewhat in Band 10, and drops to very low values in Bands 11 and 12. In the visual interpretation of the imagery, there is some indication of a decrease in reflectance in Band 7, followed by a consistent drop in reflectance in Bands 8 through 12.

No significant difference in the reflectance characteristics of snow is apparent in the five cases examined, even though two of the cases were from the late spring and the other three from mid-winter. One difference that was observed, however, is that in both of the late

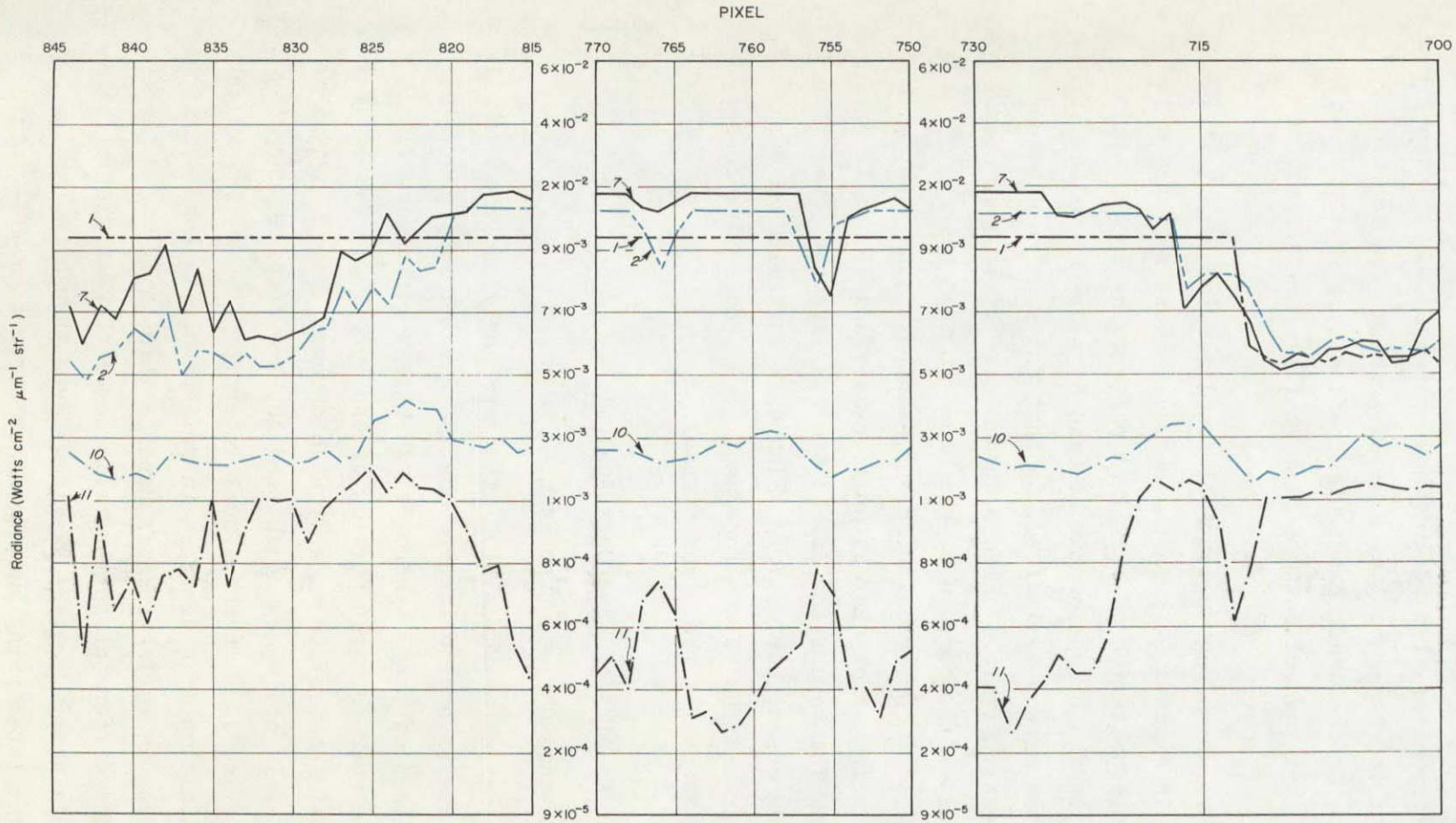

Figure 5-16 Graph showing S192 measured radiance values for selected spectral bands along a scanline crossing the Mt. Nebo Range in Utah. The profile represents radiance values measured over surface features including non-forested terrain, solid snowpack, and patchy snow.

Figure 5-17 Enlarged S190A photograph showing the Mt. Nebo Range and San Pitch Mountains in Utah. Area covered by the profile graph (Figure 5-16) is indicated.

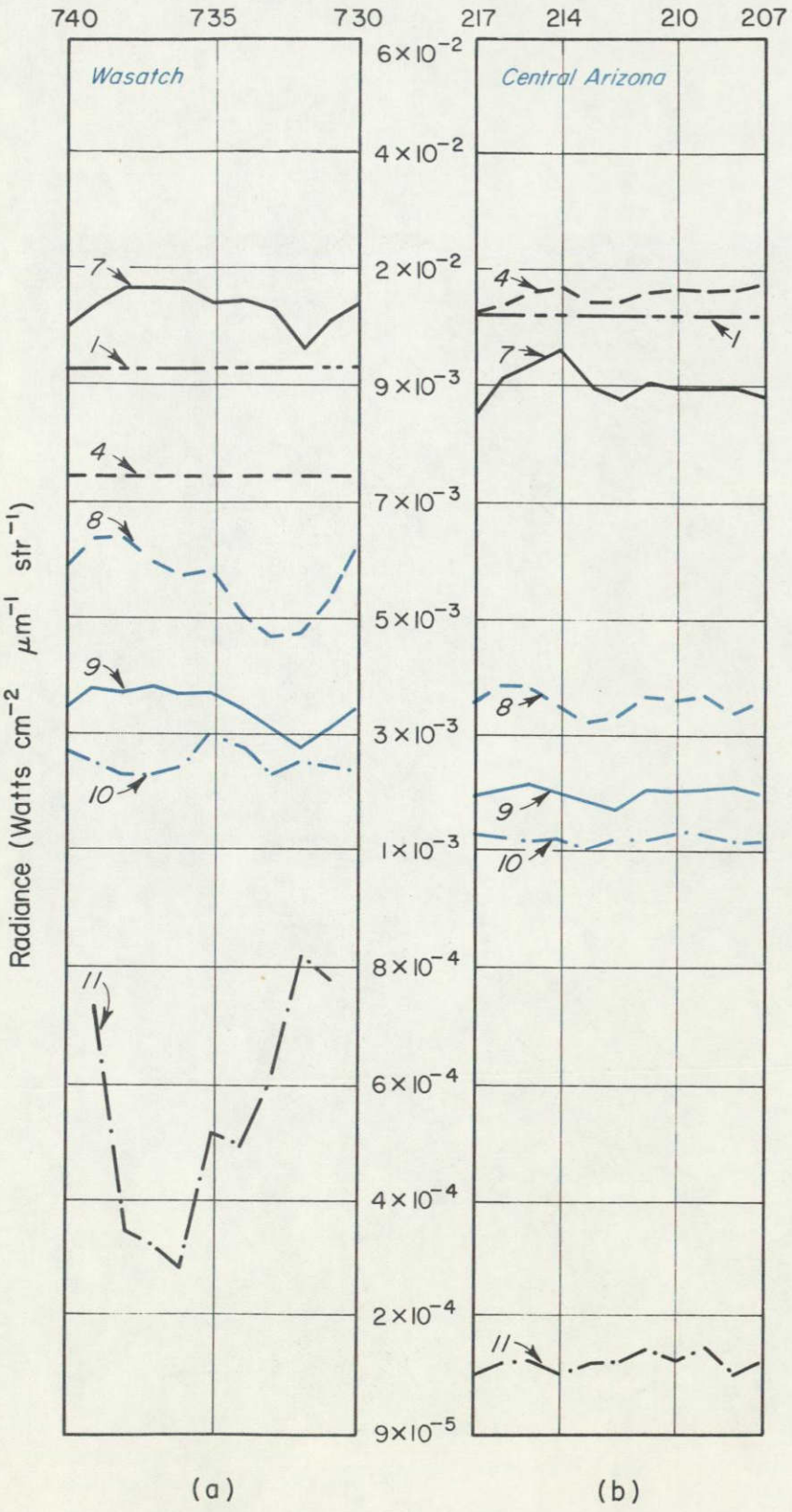

Figure 5-18 Graphs showing S192 measured radiance profiles vs. spectral band for snowcover in (a) Utah test site, (b) central Arizona test site, (c) Midwest test site, and (d) Sierra Nevada-Walker Lake test site.

751406 751407

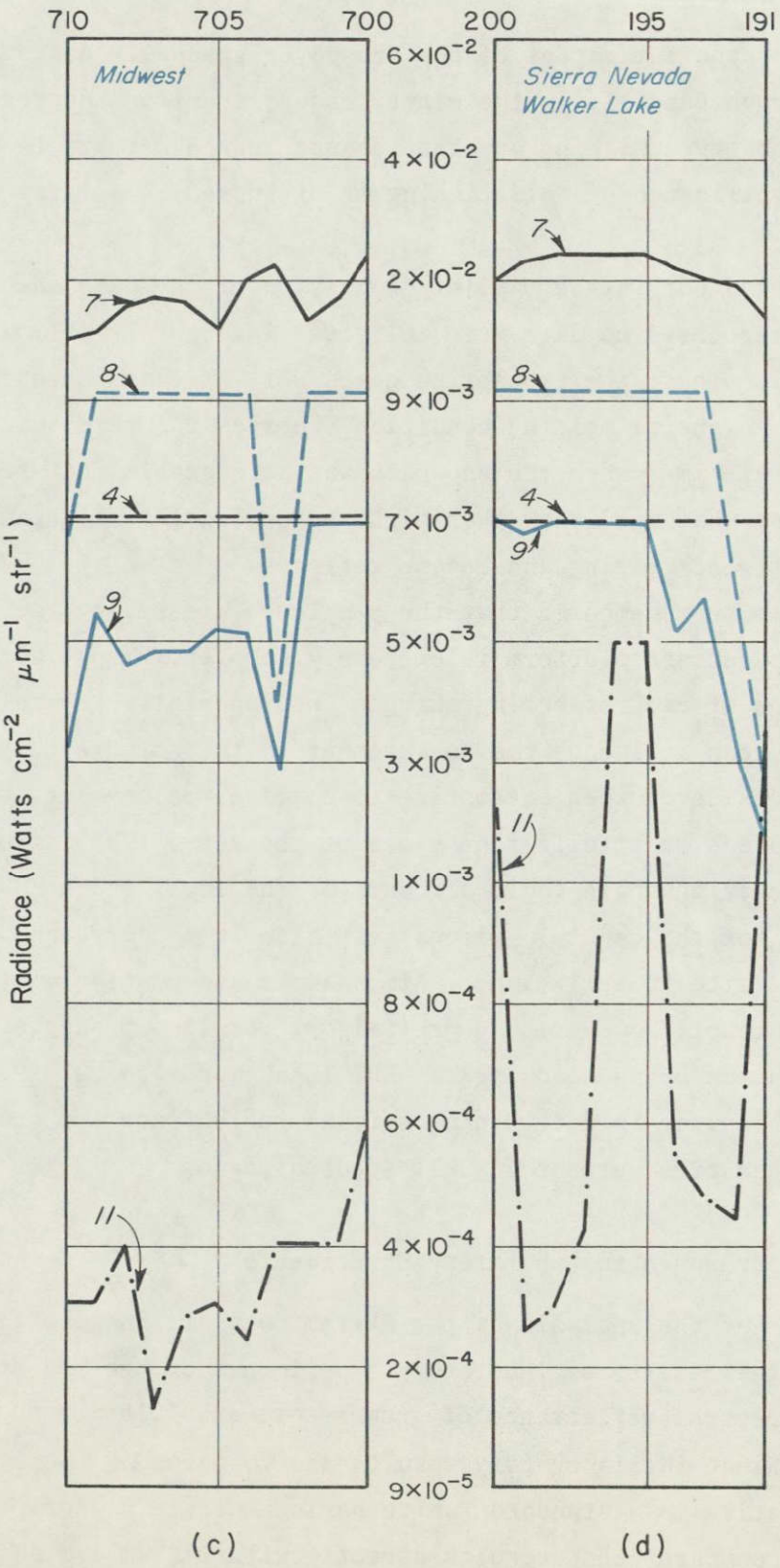

751409 751408

spring cases the apparent extent of the snowcover gradually decreases from Band 7 through Band 11; in the winter cases, a uniform decrease in reflectance is observed with no apparent change in the detectable snow extent. The significance of this finding is discussed in a later paragraph.

As was pointed out in the earlier discussion of the data sample, even in the winter cases no data were collected immediately following a fresh snowfall. Thus, the two spring cases were at times when the snowpack was in a general melting condition, whereas the three wintertime cases were at times when the snowpack was more stable but still consisting of somewhat aged snow that might be undergoing slight melting or have undergone melting and become refrozen.

It must also be remembered that the problem of measuring radiance values from a spacecraft platform is extremely complex. Many factors, such as the slope of the reflecting surface and especially the solar elevation angle, can influence the measurements. The solar elevation angle must be considered when attempting to compare measurements taken over different areas or at different times of the year. The differences in the solar elevation angle could account for the lower radiance values obtained for the central Arizona test site in January than for the Wasatch test site in early June. Atmospheric attenuation must also be taken into account; however, the preliminary results of another Skylab investigation being conducted at ERT (Chang and Isaacs, 1975) indicate that the error in determining surface reflectance for snow would be less than five percent for all spectral bands.

5.5.2 Comparison With Laboratory Experiments

The results of the analysis of the Skylab data are in general agreement with the results of laboratory experiments of the red and near-infrared spectral reflectance of snow reported by O'Brien and Munis (1973). Since the laboratory results are in terms of the snow reflectance relative to a standard (white barium sulfate powder), it is difficult to compare these results directly with S192 measured radiances. However, a graph of the laboratory results (Figure 5-19) shows similar tendencies to the S192 radiances over snowcover (Figures 5-12 and 5-13). The S192 results indicate a decrease in snow reflectance beginning in Band 8 (0.98-1.08 μm); the laboratory experiments indicate

a high reflectance in the red, with a marked decrease in reflectance from about 0.90 to 1.0 μm (a slight increase in reflectance occurs at 1.0 to 1.1 μm). Secondly, the S192 results show a slight leveling off of the drop in snow reflectance in Band 10 (1.20-1.30 μm); the laboratory experiments show that the reflectance decreases rapidly from 1.1 to 1.5 μm with the exception that at about 1.25-1.35 μm it levels off and even makes a slight recovery. Finally, the S192 results show the lowest reflectance values to be in Bands 11 (1.55-1.75 μm) and 12 (2.10-2.35); the laboratory experiments show low reflectance values at about 1.5-1.6 μm and an even stronger depression at 1.95-2.05 μm with a very slight rise at about 2.25 μm.

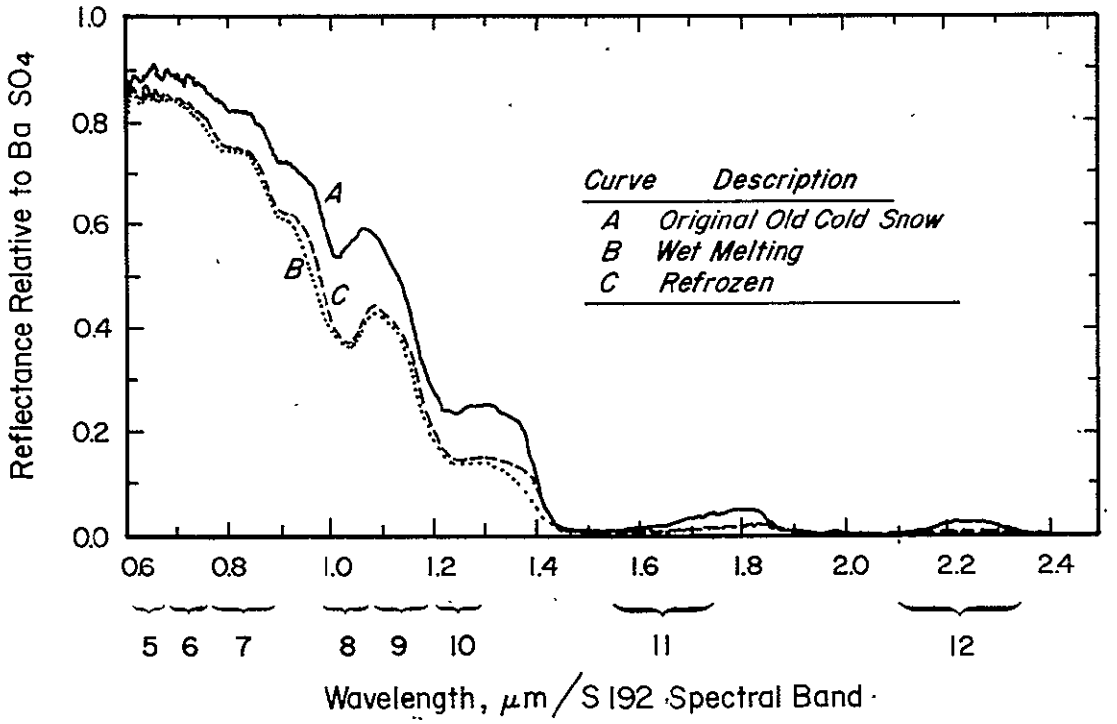

507076

Figure 5-19 Graph of laboratory results showing the effects of varying temperature conditions on the reflectance of old snow (from O'Brien and Munis, 1975).

O'Brien and Munis found that natural aging of the snow influences both the degree and rate of change of the reflectance. In general, melting lowers the reflectance, with some recovery if the snow is refrozen. A significant difference in the reflectance curves for dry and melting snow occurs at about 1.2-1.4 μm. The snowcover observed in the Skylab experiment had in each case aged to a certain extent.

The more advanced state of melting in the two late spring cases could account for the decrease in the apparent snow extent observed in the S192 imagery. In each case, it is probable that the lower elevations were undergoing more rapid snowmelt than the higher elevations at the time of the EREP Pass. Therefore, the shorter wavelength spectral bands (Bands 8, 9, and 10) will show a low reflectance where the snow is the wettest, but still a relatively high reflectance where the snow is drier, at the higher elevations. In the longer wavelengths (Bands 11 and 12), even the drier snow has a low reflectance. It is difficult to account for the progressive decrease in apparent snow extent in Bands 7 through 11, unless it is that snow wetness has a stronger influence in the shorter wavelengths than it does the longer wavelengths.

5.5.3 Snow Reflectance vs. Cloud Reflectance

A result of the analysis of the S192 data that has a significant potential application is the observed differences in the reflectance of snow and water droplet clouds. Whereas snow has a very low reflectance in the near-infrared, the water clouds remain at a high reflectance throughout the visible and near-infrared spectral regions. In a recent report by Hunt, Salisbury, and Bunting (1974), it is pointed out that a water droplet cloud displays two strong absorption bands centered at 1.41 and 1.92 μm. The spectrum of such a cloud observed from satellite altitudes will be distorted by atmospheric absorption, primarily by water vapor. The presence of these water vapor bands in the radiation received at satellite altitude will tend to distort a water cloud spectrum toward shorter wavelengths.

Snow also displays the two strong molecular vibration bands seen in spectra of liquid water and water vapor, but shifted to considerably longer wavelength. These bands lie at a sufficiently long wavelength so that they are relatively little distorted by atmospheric water vapor absorption bands. There are, of course, different kinds of snow, which yield slightly different spectra, but all have in common a very low reflectance in the 1.5-1.6 μm region as well as near 2.0 μm. Consequently, imagery made with a filter spanning either the 1.5-1.6 μm or 1.95-2.05 μm wavelength range will show snow as a dark part of the scene. Water clouds, by contrast, will remain relatively bright in both these regions, as they are in the visible. The combined use of the visible and near-infrared bands, therefore, can provide a means for distinguishing automatically between snow and water clouds. This application of the S192 data is discussed further in Section 7.

Hunt, Salisbury, and Bunting (1974) point out that the differences in the reflectance of snow and ice clouds are more complex, and that the literature does not provide much information in this area. Unfortunately, no ice clouds existed in the cases for which S192 data were available. The use of thermal infrared measurements in conjunction with the visible and near-infrared may help in distinguishing snow and ice clouds. Presumably, the cloud tops and snow surfaces would have different temperatures even though their respective reflectance characteristics may be similar (the application of thermal infrared data to snow mapping is discussed in Barnés and Bowley, 1974). Further study of the factors that could influence the use of thermal infrared to distinguish snow from ice clouds, such as differences in the emmissivities of snow and thin cirrus cloud, is recommended.

PAGE INTENTIONALLY BLANK

6. ANALYSIS OF S193 AND S194 MICROWAVE DATA

6.1 Background

Snow extent may be estimated through the use of passive microwave measurements by mapping at a sufficiently small spatial resolution where the radiation temperature of each instantaneous field-of-view (IFOV) below a certain value represents snow. Meier (1972) mapped snowcover on Mount Rainier in June 1968 with an airborne radiometer that responded to radiation at 19.35 GHz (1.55 cm). A reasonable accuracy was obtained in a comparison with snowlines traced from aerial photographs, and, for a small part of the area, extrapolated on the basis of altitude. Distributions of radiation temperature with respect to type of snow and terrain were extracted from the data. Significant differences were apparent between wet and dry snow and between snowcovered and snow free terrain despite considerable overlap in some cases. The large IFOV's of the S193 and, especially, the S194 prevent the use of this method for detailed mapping of snow, although approximate boundaries and other properties of snow (e.g. wetness) possibly may be inferred.

Meir (1972) also suggested that if the emissivities of all surfaces in the IFOV are known and reflected sky radiation is small, the percentage of snowcover in each IFOV may be estimated given only the overall radiation temperature. Presently this method of obtaining snow information cannot be utilized because the emissivities of most naturally occurring surfaces are not well understood, and the percent area of each type of terrain within the large IFOV of the S193 or S194 would be difficult to ascertain. Also wet and dry snow emit differently since emission depends on snow density and liquid water content (wetness).

One of the primary advantages of microwave radiometers is their ability to "see" through non-precipitating clouds. Unfortunately, microwave radiation, especially at longer wavelengths, passes through snow as well. Thus the temperature "seen" by the sensor may arise mostly from emission by the underlying surface material despite a snowcover. The depth of penetration of microwaves from 0.8 to 21 cm varies from < 1m to > 1.6m (Meir and Edgerton, 1971, and Edgerton et al, 1971). The penetration also varies with density and wetness of the snow; dry loose snow is

more transparent. We may assume that 2.2 and 21 cm radiation will pass through dry snow less than about 1 and 2 m thick respectively without significant attenuation. Except for relatively small areas during the winter or early spring (e.g. the Cascades), radiometers such as the S193 (about 2.2 cm) and S194 (21 cm) will measure mostly radiation emitted from the ground beneath the snow.

The radiation temperature also depends on polarization. Differences in temperature for vertically and horizontally polarized radiation at 21 cm range from about 15 to 40°K (between about 180 and 220°K) for different snow densities (Edgerton et al, 1971 and Meier and Edgerton, 1971). These differences are about 10 to 15°K (between 245 and 260°K) for 2.2 cm radiation. Measurements by Edgerton et al (1971) at 0.8 to 6 cm indicate that microwave emission also may depend on surface roughness.

6.2 Procedure of Analysis

6.2.1 S193 Data

The S193 can operate as a microwave radiometer, scatterometer, or altimeter at a frequency of 13.9 $\pm$ 0.1 GHz (wavelength $\sim$ 2.16 cm). It can view the surface from nadir to 48° perpendicular or parallel to the sub-satellite track in a continuous or stepped scan. The "half-power" IFOV at nadir is approximately a 12 km diameter circle assuming a satellite altitude of 435 km. The IFOV for reception of about 90 percent of available power is about 25 km near nadir. As a radiometer the S193 measures thermal "noise" and obtains a mean value by means of a sufficiently long observation. The possible temperature range is about 50 to 330°K with a resolution $\simeq$ 1.0°K.

One pass (EREP pass 3) of S193 data was available for analysis covering the period from 19:22:02 to 19:24:25 GMT on 3 June 1973. These data were listed in tabular form by the Flight Operations Directorate at NASA/JSC. Radiometric Antenna Temperatures (T_{RA}) in degress K were extracted from the data book and plotted in a rectangular block approximately representing the area of the data swath selected for close examination. This area encompasses several lakes, Mono, Tahoe, and Walker, and includes the White Mountains and a portion of the Sierra Nevada (see figure 2-2). The centerline of this section of Pass 3 runs

approximately from 39.6°N, 121.0°W to 37.4°N, 117.1°W. The four "corners" of this section are delineated roughly by the following coordinates:

Corner	Lat (°N)	Long (°W)
Upper Left	39.0	121.4
Upper Right	40.2	120.6
Lower Left	36.8	117.6
Lower Right	37.9	116.7

The temperatures were analyzed as shown in Figure 6-1 by drawing the 200, 250, 260, 270, 275, and 280°K isotherms. The 275°K isotherm was drawn as a dashed line, the others were drawn as solid lines. Areas having a $T_{RA} \geq 280°K$ were stippled, those with $T_{RA} \leq 250°K$ were hatched, and the one area where $T_{RA} \leq 200°K$ was cross-hatched. Geographical landmarks are labeled at their approximate locations. Note that there was about a 50 percent overlap between adjacent scan spots for the half-power IFOV of about 12 km near nadir. Overlap was determined by comparing geographical coordinates of centers of adjacent scan spots listed in the data book.

6.2.2 S194 Data

The S194 (L-Band) radiometer operates at 1.4 to 1.427 GHz ($\sim$ 21 cm) and has roughly a rectangular IFOV of about 285 km (154 nmi) that encompasses more than 90 percent of received radiant energy with about half the energy from a smaller area of about 124 km (67 nmi) on a "side". The radiant energy is sampled at a rate that ensures at least a 97 percent ground coverage overlap. The possible temperature range is about 0 to 350°K with a resolution of $\pm$ 1.0°K.

Differences between snowcovered and snow free surfaces may appear in the S194 data since at least part of the radiation from snowcovered terrain should arise from the snow. Four cases were analyzed to determine if any useful information on snow could be extracted from the S194 data in their tabulated form (i.e. radiation temperatures). The four cases examined were extracted from data books provided by the Flight Operations Directorate, and were as follows:

Case	Pass	Approximate Location	Median Time(GMT)	Date
1)	83	Northern Plains	17:03:15	14 Jan. 1974
2)	83	Salt Verde Watershed	16:59:12	14 Jan. 1974
3)	89	Upper Mid-West	17:59:00	24 Jan. 1974
4)	98	Sierra Nevada	16:59:25	1 Feb. 1974

The first case was an attempt to estimate the mean radiation temperature for an extensive snowcovered region of relatively flat relief in the northern plains of the United States. In all, 36 consecutive values were averaged representing an area approximately 200 km wide and 300 km long.

For the second case (Figure 6-2a) every third scan spot was plotted extending along a line from about 34.0°N, 113.0°W to 35.6°N, 110.7°W. Adjacent plotted points have an overlap of about 90 percent. Figure 6-2b (third case) is a plot of every 12th scan spot along a line from about 42.3°N, 92.3°W to 38.9°N, 85.6°W. The overlap is about 65 percent. Figure 6-2c (fourth case) is a section from about 40.1°N, 121.0°W to 37.3°N, 116.2°W where each plotted value is an average of three spots centered at every tenth spot (i.e. the 9th, 10th, and 11th scan spots are averaged and plotted as the tenth spot). The overlap between plotted values is about 75 to 80 percent. Note that the ground resolution of these average values differs by no more than about 10 percent of that of a single scan spot (about 313 vs. 285 km) because of the 97 percent overlap of adjacent scan spots.

6.3 Discussion of Results

6.3.1 S193 Results

Figure 6-1 suggests that the primary factor in determining the radiometric temperature at 13.9 GHz is the emissivity of the surface as indicated by the low temperatures for the three lakes, especially the largest, Lake Tahoe (T_{RA} < 200°K). A water surface at this frequency has a radiometric temperature of about 110°K. However, a view only of the water surface of one of these lakes is not possible because

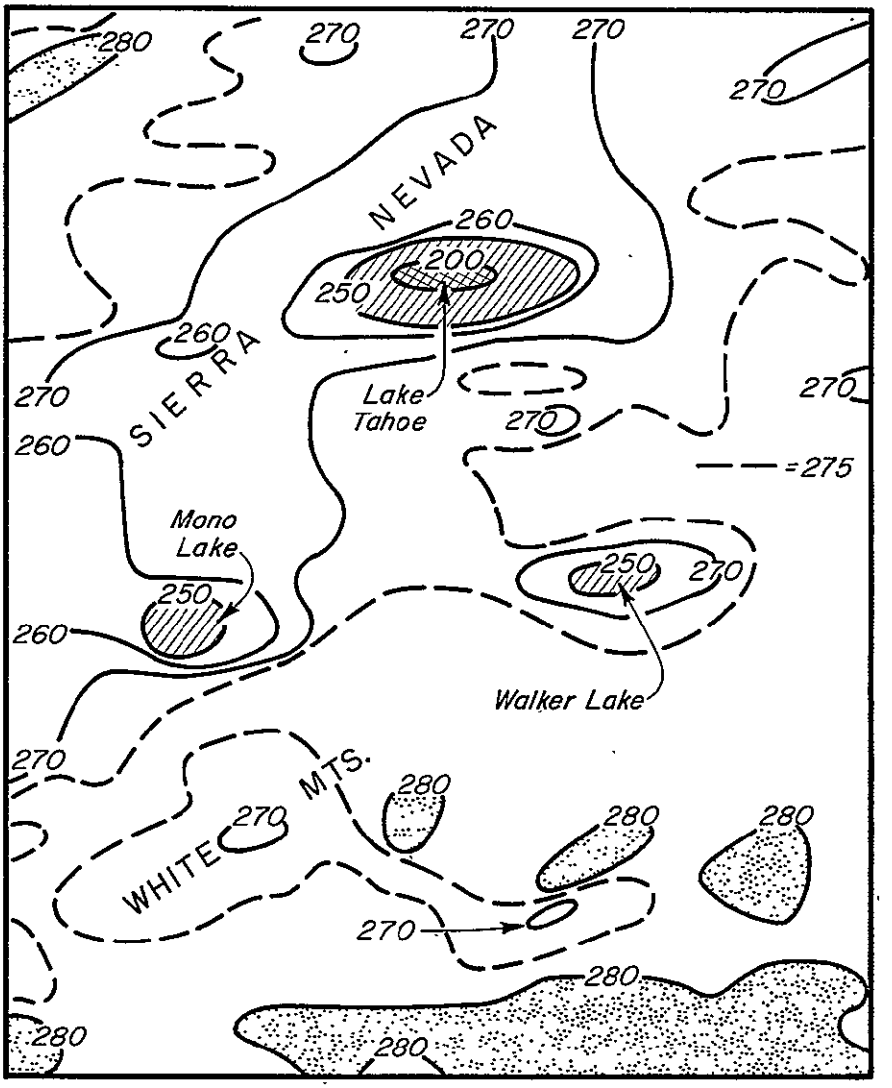

Figure 6-1 S193 radiometric antenna temperature (°K) from EREP Pass 3 on 3 June 1973.

of the large overall IFOV of the S193; values of $T_{RA} < 250°K$ represent a mixture of land and water surfaces.

Mountainous regions also exhibit lower temperatures than generally found in the rest of the observed area, except those for the lakes, suggesting some dependence on thermal temperature. In this case, thermal temperature of a "surface" refers to depths of from a few cm to more than 1 m for dry snow. However, thermal temperature appears less important than emissivity, as seen by comparing the lowest non-water values with those for Lake Tahoe.

In Figure 6-1 information on snow cannot be separated from that on height since extent of snowcover closely parallels extent of terrain over a certain height. For example, the area of lower T_{RA} ($\leq 260°K$) to the northwest of Mono Lake has an extensive snowcover, but it is also an area of comparatively high terrain. The rough delineation of snow boundaries may be possible for relatively flat country, but only for deep snow (e.g. 5 or 10 cm of snow may be nearly transparent to 13.9 GHz radiation).

The S193 radiometer does not appear to be useful as an instrument for mapping snow because of the following:

(a) the large IFOV of about 25 km for about 90 percent of received energy,

(b) the large penetration depth of > 1 m for 13.9 GHz (2.16 cm) radiation, and

(c) a "mixed" dependence of the radiometric temperature on emissivity and thermal temperature, with emissivity apparently dominating.

Nevertheless, a future microwave radiometer of this type could be useful for inferring properties of snow as well as delineating boundaries, especially for relatively flat terrain. Use of a shorter wavelength, say 0.8 cm, and a smaller IFOV would increase the utility of such an instrument. Further study is required on the microwave properties of snow and other materials to determine optimum frequency for determining snow boundaries and properties (e.g. water content or thickness). If the emissivities of snowcovered and snow free terrain are known to a sufficient accuracy snow extent within a single IFOV may be estimated given only T_{RA}. More than one frequency would be required for more than

one type of snow (see Meier, 1972). Further study into this latter method also should be pursued.

6.3.2 S194 Results

The mean radiation temperature for the first case (Pass 83, Northern Plains) was 240.3°K with individual values running from 239.5 to 243.7°K. This temperature is about 20°K or more higher than those presented by Edgerton et al (1971), suggesting that the radiometer viewed the ground as well as the overlying snow. In general, snow depths for that area (southeast corner of South Dakota) were less than 0.5 m, most often about 10 to 20 cm, as reported in climatological data books.

Figure 6-2a extends across the Salt Verde watershed in central Arizona. High and snowcovered terrain is associated with a region of higher radiation temperature on the figure, suggesting that the primary cause of this feature was a higher emissivity of the snow and/or underlying material. These temperatures roughly agree with those of the first case.

The third case, Figure 6-2b, represents a swath whose centerline runs to within about 150 km of the southern end of Lake Michigan. Even though the lake is barely within the overall IFOV of the sensor (including radiation from beyond the half-power "width") the extremely low radiometric temperature of a water surface, about 95°K, apparently resulted in the observed decrease. The decrease in radiation temperature reached its maximum at the closest point of approach of the sensor to the lake. Note that temperatures at the extreme left of Figure 6-2b are similar to those of the first case and the "high terrain" part of Figure 6-2a.

Figure 6-2c represents a swath across the Sierra Nevada, passing over Walker Lake. The lake should have little effect on the sensed temperature because of its small size relative to the IFOV of the S194. The lake is 10 km wide and 30 km long compared with an IFOV of about 285 km. Nevertheless, the presence of this lake apparently causes a slight dip in the temperature curve, but a definite statement cannot be made. In this last case only a small percent of the area had a snowcover, but the radiation temperatures for the higher terrain are closely similar to those of the first two cases and the extreme left of

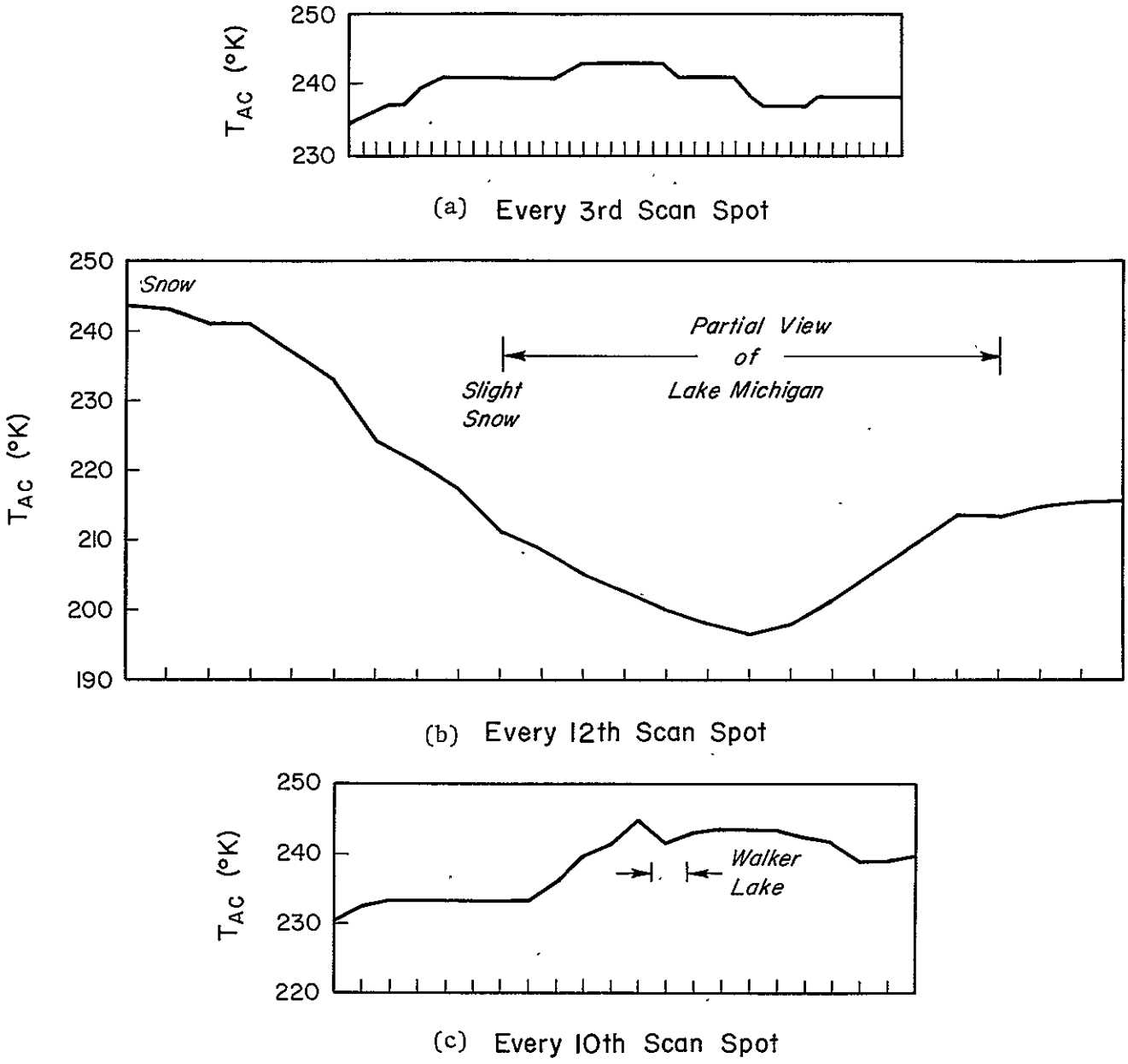

Figure 6-2 S194 corrected antenna temperature (T_{AC}) for EREP Pass 83 on 14 January (6-2a), 89 on 24 January (6-2b), and 98 on 1 February (6-2c). See text, Section 6.2, for further details on location of these passes. In Figure 6-2c, each plotted point is an average of three adjacent scan spots.

Figure 6.2b. These similarities suggest that, (1) the higher values represent an effect of the emissivity of the higher terrain relative to that of the lower ground, and (2) snow emissivity causes the observed higher temperatures. This apparent contradiction cannot be sorted out with the available data. However, it is evident that for most snow-covered terrain, depths < 1 m, the ground emissivity determines the greater part of the observed radiation.

The results of this section can be summarized by stating that the S194 radiometer is not useful for mapping snow given the large IFOV of the instrument and the lack of a detailed knowledge of the emissivity of various terrain types in each IFOV. Even if these deficiencies were corrected an L-band radiometer could only be used to map snow greater than about 2 m deep. Snow of such depths comprises only a small portion of total snowcover except in certain mountainous regions.

PAGE INTENTIONALLY BLANK

7. CONCLUSIONS

To investigate the utility of Skylab EREP data for mapping snowcover, data were collected for five test site areas, four of which were in mountainous areas of the western United States and one in the Upper Mississippi-Missouri River Basins area in the Midwest. The data were collected on three EREP passes on the SL-2 mission in June 1973 and on four EREP passes on the SL-4 mission in January-February 1974. The investigation included analysis of S190A and S190B photography, S192 film and digital data, and S193 and S194 digital data. The conclusions based on the results of the analysis of the Skylab EREP data sample are presented in the following paragraphs.

7.1 Utility of S190A and S190B Photography

The results of the analysis of S190A and S190B photography from the SL-4 mission support the conclusions based on the preliminary analysis of the data sample from the SL-2 mission. Photography from the Multispectral and Earth Terrain Cameras can be used to obtain accurate mapping of snowcover extent and detailed characteristics of features within snowcovered areas. In comparison with aerial snow survey charts, the snowline can be mapped in greater detail and can be positioned more precisely using the Skylab photographs; greater detail can also be mapped from the Skylab photographs than from Landsat-1 imagery; in fact, it appears that as much detail in snowcover extent can be mapped from the S190B photography as from high-altitude aircraft photography. The color products facilitate the interpretation of snowcover, and the color-infrared photographs offer some advantages over the aerial color photographs with regard to detecting snow in vegetated areas.

Because of the nature of the data sample it was possible to compare the Skylab photography with Landsat imagery and other snow data only for the few specific times of the EREP passes. It was not possible to assess the utility of these data over an entire snowmelt season, and, therefore, to determine whether the greater detail that can be mapped from Skylab photography would offer significant improvement for snow hydrology purposes over a satellite system with the resolution of

Landsat. For operational snow mapping programs satellite observations covering extensive areas on a regular basis are needed; therefore, a somewhat lower resolution system that can provide frequent coverage may be more useful. Similarly, for operational snow mapping the advantages of color photography may not be sufficient to justify the added cost.

High resolution color photography, of the quality of the S190B Earth Terrain Camera, would be advantageous for monitoring limited areas during critical periods, such as in times of high-flood potential. Frequent repetitive coverage, perhaps as possible in a space shuttle mode of operation, would be necessary. The results of the data analysis also indicate that the high resolution photography has application to monitoring environmental changes and updating maps. In this application, such as for monitoring the extent of forest-cutting operations, the existence of snow on the ground greatly facilitates the interpretation, and may, in fact, be essential.

The S190A and S190B photography provided a completely adequate means for mapping snowcover in support of the analysis of data from the other EREP sensors. The precise definition of the snowcovered areas could not have been obtained by any other means. The aircraft photography collected in support of the Skylab experiment was extremely useful in evaluating the utility of the S190A and S190B photography; the aircraft data were not essential, however, in the analysis of the measurements from the other EREP sensors.

7.2 Utility of S192 Data

The results of the Skylab EREP investigation that have the greatest significance to snow mapping are the results of the analysis of the S192 Multispectral Scanner data. Whereas the results of the analysis of the S190A and S190B photography essentially demonstrate the utility of improved camera systems operating in spectral regions for which earlier observations had been available, the S192 data provided for the first time the opportunity to examine from a spacecraft the snow reflectance characteristics in several distinct spectral bands extending into the near-infrared as far as the 2 μm region.

The principal result of the analysis of S192 data is the decrease in the reflectance of snow in the near-infrared. The observed decrease

in reflectance is consistent in both the film products and magnetic tape data for the EREP passes for which data were collected. Snow reflectance remains high in the visible, begins to decrease in Bands 7 and 8 (0.78 - 0.88 μm and 0.98 - 1.08 μm respectively), and drops dramatically in Bands 11 and 12 (1.55 - 1.75 μm and 2.10 - 2.35 μm, respectively); in the latter two bands, snowcover appears essentially black in the S192 film products. The snow reflectance characteristics in the Skylab data are in close agreement with the results of laboratory experiments reported by other investigators.

Based on the results of the analysis of S192 data, two potential applications to snow mapping of measurements in the near-infrared spectral region are possible: (1) the use of a near-infrared band in conjunction with a visible band to distinguish automatically between snow and clouds; and (2) the use of one or more near-infrared bands to detect melting snow.

The nearly complete reversal in snow reflectance between the visible bands and Bands 11 and 12 observed in each case indicates that in this portion of the near-infrared, snow surfaces are essentially non-reflective regardless of the condition of the snow. In contrast, the reflectance of clouds (water droplet) is essentially the same in each of the S192 bands, displaying no drop in the near-infrared. As a result, a technique combining two spectral bands, one in the visible and one in the near-infrared at the position of Band 11 or 12 (1.55 - 1.75 μm or 2.10 - 2.35 μm), can be used to distinguish between snow, clouds, and non-snowcovered ground. A feature having a high reflectance in the visible and a low reflectance in the near-infrared would be classified as snow; a feature having a high reflectance in both bands would be classified as cloud; and a feature having a low reflectance in the visible and a medium reflectance in the near-infrared would be classified as non-snowcovered ground. An automatic technique for distinguishing snow from clouds is of particular significance, since this has been recognized as a serious problem with regard to the eventual machine processing of satellite data for snowcover mapping.

The second potential application, that of detecting melting snow, is based on the observed behavior of snow in the intermediate bands

from about Band 7 (0.78 - 0.88 μm) through Band 10 (1.20 - 1.30 μm). Although the data sample was not optimum in that no data were collected over fresh, cold snow surfaces, the S192 film products for the spring cases (June 1973) display snow reflectance characteristics not observed in the winter cases (January-February 1974). In the two spring cases, the apparent snow extent decreases gradually from a maximum in the visible (Band 6) to a miminum in Band 11. This gradual decrease in the area of high reflectance is difficult to account for unless it is because the snow at the lower elevations is melting, and therefore exhibits a more rapid drop in reflectance, whereas the snow at the highest elevations is dryer or refrozen, and therefore does not exhibit a significant drop in reflectance until Band 11 (1.55 - 1.75 μm). In the winter cases, the snowpack is more uniform at all elevations, so does not display the gradual reduction in the area of high reflectance. It is concluded, therefore, that bands in the spectral range from about 0.8 μm to about 1.30 μm should provide the most information on the condition of the snow surface with regard to the snow being in a melting (wet surface) or a non-melting or refrozen condition (dry surface).

7.3 Utility of S193 and S194 Data

The results of the analysis of data from the S193 Radiometer/Scatterometer and the S194 L-Band Radiometer are not conclusive with regard to the utility of these sensors for snow mapping. Only a very limited sample of S193 data was available for analysis; although the locations of lakes and the mountain ranges could be mapped from the brightness temperatures, it was not possible to correlate the measured temperatures to specific areas of snowcover. Similarly, because of the gross field of view of the S194 sensor, the brightness temperatures mapped for the three EREP passes could not be correlated with the snowcover as mapped from the S190A photography.

Aside from problems of too-large a field-of-view and limited quantities of data, the difficulty in interpreting the results as a consequence of the high transmissivity of snow in the microwave spectral region must be taken into account. Snow of depths less than about 1 or 2 meters is nearly transparent to 13.9 GHz or 1.4 GHz radiation

respectively; only a few mountainous regions commonly have a snowcover of greater depth. Therefore, in most cases a microwave radiometer similar to the S193 or S194 would effectively measure emission from the underlying ground, whose emissivity may vary considerably from place to place, thereby greatly overwhelming any changes arising from the presence of snow. Over flat relatively uniform terrain snow depths of 10 to 30 cm are most common, only occasionally exceeding 50 cm in the United States, thereby making doubtful the effectiveness of a radiometer sensitive to 2.2 or 21.0 cm radiation. It is possible that a future radiometer having a smaller field of view and operating at 19.4 GHz or a higher frequency may prove more useful for snow mapping.

7.4 Assessment of Operational Utility and Cost Benefits of Results

In order to assess properly the operational utility and cost b[illegible] of the results of the investigation, it would be necessary to examine a data sample for several drainage basins over a complete snowmelt season. However, the results of the analysis of the available data sample further demonstrate the utility of spacecraft data for snow mapping. Moreover, since the data were analyzed for various test site areas, there appears no reason why the analysis techniques could not be extended to other areas of the United States or the World where snow hydrology is a concern.

The results of the analysis of the Skylab EREP S192 data have particular significance and potential cost-saving application to snow mapping. First, the combined use of visible and near-infrared measurements to distinguish between snow and clouds is a potential cost-saving application because it will enable further development of automatic snow mapping techniques; the need for an analyst to distinguish snow from clouds subjectively will be greatly reduced. Furthermore, a method to distinguish snow from clouds through machine processing will also be of benefit in the preparation of cloud analyses using satellite data. Second, the timeliness and accuracy of input to snowmelt runoff models will be increased with knowledge of the locations and extent of areas where the snowcover is in a melting condition; snowmelt information is particularly needed in regions such as the Salt-Verde Watershed in Arizona where significant portions of the snowpack can melt completely within a few days or even hours.

It is realized, however, that further study of snow reflectance characteristics is needed. The available data sample did not include a situation where snow and ice clouds are present, where the technique to distinguish between snow and water droplet clouds could be tested to determine its application to ice clouds; also, measurements over fresh, dry snow as well as additional measurements over areas of known melting snow are needed before the relationships between reflectance and snow condition are completely understood.

Nevertheless, the results of the analysis of Skylab EREP data are believed to be sufficiently conclusive to warrant careful consideration for including one or more near-infrared spectral bands on radiometers to be flown on future operational satellite systems. Measurements in the near-infrared spectral region, in combination with visible and thermal infrared measurements, have the potential for providing greatly improved information with regard to snow hydrology and thus have the potential for providing eventual significant cost savings to snow survey programs.

8. REFERENCES

Aerospace and Defense Systems Operations, 1973: Earth Resources Production Processing Requirements: EREP Electronic Sensors; Document No. PHO-TR524 prepared by Philco Ford Corp. for NASA/Johnson Space Center, Houston, Texas.

Barnes, J. C., and C.J. Bowley, 1970: The Use of Environmental Satellite Data for Mapping Annual Snow-Extent Decrease in the Western United States, Final Report, Contract No. E-252-69(N), Allied Research Associates, Inc., Concord, MA, 116 pp.

Barnes, J.C., and C.J. Bowley, 1974: Handbook of Techniques for Satellite Snow Mapping, Report prepared under Contract NAS 5-21803, Environmental Research & Technology, Inc., Concord, MA, 95 pp.

Barnes, J.C., C.J. Bowley, J.T. Parr, and M.D. Smallwood, 1975: Skylab-4 Visual Observations Project: Snow Mapping Experiment, Final Report, Contract No. NAS 9-13974, Environmental Research & Technology, Inc., Concord, MA, (in publication).

Barnes, J.C., C.J. Bowley, and D.A. Simmes, 1974: The Application of ERTS Imagery to Mapping Snowcover in the Western United States, Final Report under Contract NAS 5-21803, Environmental Research & Technology, Inc., Concord, MA, 77 pp.

Barnes, J.C., C.J. Bowley, and M.D. Smallwood, 1974: A Study to Develop Improved Spacecraft Snow Survey Methods Using Skylab/EREP Data: Demonstration of the Utility of the S190 and S192 Data, Interim Report under Contract NAS 9-13305, Environmental Research & Technology, Inc., Concord, MA, 51 pp.

Bowley, C.J., and J.C. Barnes, 1975: The Application of ERTS Imagery to Mapping Snowcover in the Western United States, Supplemental Report under Contract NAS 5-21803, Environmental Research & Technology, Inc., Concord, MA, 43 pp.

Brown, H.E., M.B. Baker, Jr., J.J. Rogers, W.P. Clary, J.L. Kovner, F.R. Larson, C.C. Avery, and R.E. Campbell, 1974: Opportunities for Increasing Water Yields and Other Multiple Use Values on Ponderosa Pine Forest Lands, USDA For. Serv. Res. Papers RM-129, Rocky Mt. For. and Range Exp. Stn., Fort Collins, Colorado, 36 pp.

Chang, D.T. and R.G. Isaacs, 1975: "Experimental Evaluation of Atmospheric Effects on Radiometric Measurements Using the EREP of Skylab", Final Report, Contract No. NAS9-13343, Environmental Research & Technology, Inc., Concord, MA, (in preparation).

Clary, W.P., M.B. Baker, Jr., P.F. O'Connell, T.N. Johnsen, Jr., and R.E. Campbell, 1974: Effects of Pinyon-Juniper Removal on Natural Resource Products and Uses in Arizona, USDA For. Serv. Res. Pap. RM-128, Rocky Mt. For. and Range Exp. Stn., Fort Collins, Colorado, 28 pp.

Edgerton, A.T., Stogryn, A., and Poe, G., 1971: Microwave Radiometric Investigations of Snowpacks, Final Report, U.S. Geol. Surv., Contract No. 14-08-001-11828, Aerojet-General Corp., 81 pp.

Hunt, G.R., J.W. Salisbury, and J.T. Bunting, 1974: Distinction Between Snow and Cloud in DMSP Satellite Imagery: A Preliminary Report, unpublished report, Terrestrial Sciences Laboratory, Air Force Cambridge Research Laboratory, Hanscom AFB, MA, 15 pp.

McClain, E.P., 1973: Snow Survey from Earth Satellites, World Meteorological Organization, WMO Pub. No. 353, Geneva, 42 pp.

McGinnis, D.F., J.A. Pritchard, and D.R. Wiesnet, 1975: Snow Depth and Snow Extent Using VHRR Data from the NOAA-2 Satellite, NESS Technical Memorandum, NOAA/National Environmental Satellite Service, Suitland, MD, (in publication).

Meier, M.F., 1973: "Application of ERTS Imagery to Snow and Glacier Hydrology", paper presented at Symposium on Approaches to Earth Survey Problems Through the Use of Space Techniques, COSPAR, Konstanz.

Meier, M.F., 1972: "Measurement of Snowcover Using Passive Microwave Radiation," International Symposia on the Role of Snow and Ice in Hydrology; Symposium on Measurement and Forecasting, 13 pp.

Meier, M.F. and A.T. Edgerton, 1971: "Microwave Emission from Snow - A Progress Report," Proc. Seventh Intern. Symp. Remote Sensing of Environ., Ann Arbor, Mich., 1155-1163.

Mission Requirements and Operations Team, 1973: Skylab Program EREP Investigators' Information Book, prepared by Principal Investigations Management Office, Science and Applications Directorate, NASA/Johnson Space Center, Houston, Texas.

NASA, 1974: Skylab Earth Resources Data Catalog, Doc. No. JSC-09016, NASA/Johnson Space Center, Houston, Texas, 359 pp.

O'Brien, H.W., and R.H. Munis, 1975: Red and Near-Infrared Spectral Reflectance of Snow, Research Report 332, U.S. Army Cold Regions Research and Engineering Laboratory, Hanover, N.H., 18 pp.

Rango, A., V.V. Salomonson, and J.L. Foster, 1975: Seasonal Streamflow Estimation Employing Satellite Snowcover Observations, Preprint X-913-75-26, NASA/Goddard Space Flight Center, 34 pp.

Strong, A.E., E.P. McClain, and D.F. McGinnis, 1971: "Detection of Thawing Snow and Ice Packs through the Combined Use of Visible and Near-Infrared Measurements from Earth Satellites", Monthly Weather Review 99(11), pp. 828-830.

Wiesnet, D.R., 1974: "The Role of Satellites in Snow and Ice Measurements", Proceedings of Interdisciplinary Symposium on Advanced Concepts and Techniques in the Study of Snow and Ice Resources, National Academy of Sciences, Monterey, California, December 2-6, 1973, pp. 447-456.

C-2


SEP 1975
RECEIVED